Antarctic Science 9 (3): 313–335 (1997)

A metamorphic perspective on the Pan African overprint in the Amery area of Mac. Robertson Land, East Antarctica

IAN SCRIMGEOUR[1] and MARTIN HAND

Department of Geology and Geophysics, University of Adelaide, Adelaide, SA 5005, Australia
[1]Current Address: Northern Territory Geological Survey, PO Box 2655, Alice Springs, NT 0871, Australia

Abstract: The Amery area of Mac. Robertson Land lies between the early Palaeozoic granulite terrain of Prydz Bay and Meso-Neoproterozoic granulites in northern Prince Charles Mountains (nPCM). In contrast to the nPCM which shows an apparently simple near-isobaric history, granulites exposed in the Amery area contain reaction textures suggesting a more complex evolution. Peak-M_1 Mesoproterozoic assemblages formed at *c.* 700 MPa and 800°C and initially underwent a near-isobaric cooling. A subsequent increase in temperature (M_2) resulted in the formation of cordierite-spinel assemblages at ~450 MPa and 700°C in metapelite. The timing of M_2 is not firmly established, however existing data strongly suggest it is an early Palaeozoic event coeval with tectonism in Prydz Bay to the north-east. Thus the metamorphic evolution of granulites in the Amery area reflects a terrain-scale thermal interference pattern between two unrelated orogenic events. In rocks not recording post-M_1 isobaric cooling, the superposition of M_2 on M_1 assemblages resulted in the formation of M_2 cordierite-spinel symplectites at the expense of peak M_1 garnet and sillimanite. This texture, commonly interpreted to reflect near-isothermal decompression, has no relevance in terms of a single tectonothermal event in the Amery area.

Received 17 February 1997, accepted 4 June 1997

Key words: decompression, East Antarctica, medium-P granulites, metapelite, Pan-African, terrain reworking

Introduction

Until recently, much of the East Antarctic Shield was believed to comprise a single Proterozoic high grade metamorphic terrain separating Archaean cratonic blocks. Numerous studies throughout this terrain proposed that it underwent granulite facies metamorphism during a single major event at *c.* 1000 Ma (e.g. Harley & Hensen 1990). However, recent studies around Lutzow-Holm Bay and in Prydz Bay (Shiraishi *et al.* 1994, Zhao *et al.* 1992, 1995, Hensen & Zhou 1995, Carson *et al.* 1996, Fitzsimons 1996, Hand & Kinny 1996, Fitzsimons *et al.* 1997) have provided clear evidence for the existence of extensive Pan-African (*c.* 500 Ma) granulite terrains in the East Antarctic Shield, often with little or no evidence of an earlier 1000 Ma high grade event. In contrast to these extensively reworked areas, the northern Prince Charles Mountains (nPCM) (Fig. 1) appear to represent one region of the east Antarctic Shield where the effects of 1000 Ma tectonism are relatively well preserved (e.g. Tingey 1982, Mikhalsky *et al.* 1992, Kinny *et al.* 1997). In this region, peak metamorphic conditions of 600–700 MPa and 800°C were followed by near-isobaric cooling (Fitzsimons & Thost 1992, Thost & Hensen 1992, Fitzsimons & Harley 1994a, 1994b, Nichols 1995). This contrasts sharply with the Amery area (e.g. Jetty Peninsula) at the eastern extremity of the nPCM where a more complex evolutionary history involving cooling and heating intervals during exhumation has been proposed (Hand *et al.* 1994a).

In this paper, we describe reaction textures in granulites from the Amery area, and the eastern margin of the nPCM, encompassing an area of approximately 12 000 km^2. The peak assemblages in metapelitic rocks, and subsequent P–T evolution are modelled in the system KFMASH. P–T estimates are calculated using specific thermobarometers and the average pressure approach of Powell & Holland (1988, 1994). These data provide an insight into the thermal and baric evolution of this poorly documented terrain and provide evidence for metamorphic reworking over a substantial region. The observations further serve to highlight some of the problems in deducing P–T paths from reaction textures in high grade rocks.

Regional geology

The Amery area forms the eastern end of the nPCM, dominated by medium pressure granulite facies gneisses that grade southward into amphibolite facies rocks (Fig. 1). Within the nPCM, the Porthos and Aramis ranges are dominated by felsic orthogneiss (Fitzsimons & Thost 1992), with metasedimentary rocks more common in the Athos Range and Stinear Nunataks (Tingey 1982), Jetty Peninsula (Hand *et al.* 1994b) and in the nunataks south-west of the Aramis Range (Nichols 1995). Syn-tectonic granite, charnockite and leucogneiss intrusions occur throughout the nPCM (Tingey 1982, Fitzsimons & Thost 1992, Sheraton *et al.*

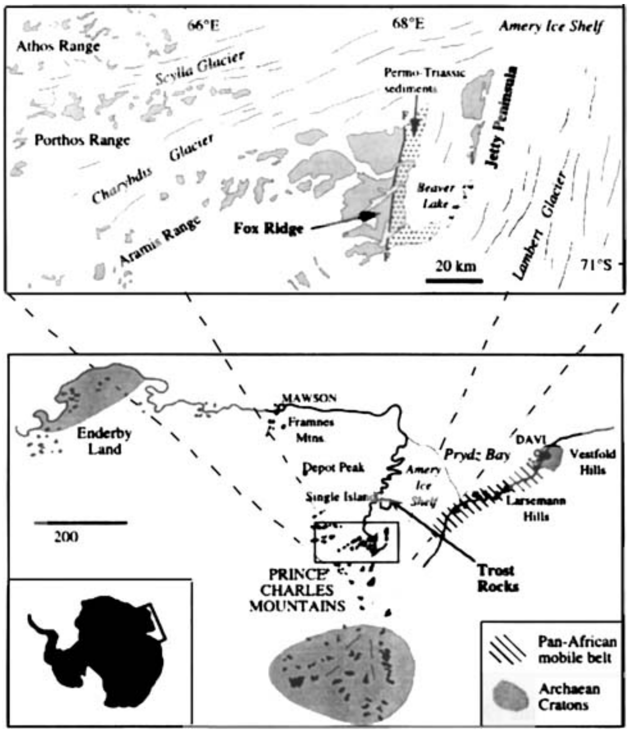

Fig. 1. Map of the Amery area showing the location of the outcrops discussed in the text and their geographic relationship to the nPCM. The distribution of Archean cratons and early Palaeozoic granulite metamorphism is shown. Remaining outcrops represent the 1000 Ma granulite terrain. Mawson and Davis refer to Australian Antarctic bases.

1996, Kinny *et al.* 1997), and minor pegmatites and rare granitic dykes postdate the majority of the high grade deformation (Fitzsimons & Thost 1992, Hand *et al.* 1994b).

Several recently published descriptions of the geological relationships in the nPCM (Fitzsimons & Thost 1992, Hand *et al.* 1994b, Kamenev *et al.* 1993, McKelvey & Stephensen 1990) result in a variety of nomenclature for the geological evolution of the region (Table I). In this paper we adopt a relatively simple scheme concentrating only on the major structural features. High-grade metamorphism was synchronous with deformation, and all gneissic rocks contain an intense layer-parallel composite foliation, S_{1-2} that formed at *c.* 1000 Ma (Arriens 1975, Tingey 1982, Manton *et al.* 1992, Kinny *et al.* 1997). A subsequent phase of deformation (D_3) produced upright E–W trending folds. Intensification of strain on the limbs of these folds resulted in the development of east–west trending steeply dipping high-strain zones, which are locally up to a kilometre wide. Extensive charnockites intruded throughout the nPCM at 980±20 Ma and have been variably deformed by D_3 (Kinny *et al.* 1997).

On Jetty Peninsula, transitional granulite grade D_4 high strain zones up to 500 m wide contain south-east-plunging lineations and show north vergent reverse movement (Hand *et al.* 1994b). Elsewhere in the nPCM (e.g. Fox Ridge), smaller scale (< 50 m) zones possibly equivalent to D_4 appear to be associated with broadly NW-up movements (Nichols 1995). Metre-scale amphibolite facies D_5 mylonites and associated pegmatite veins truncate D_4 zones (Fitzsimons & Thost 1992, Hand *et al.* 1994b, Nichols 1995). The age of D_4 and D_5 is somewhat uncertain. However monazite and zircon U-Pb geochronology on Jetty Peninsula indicates early Palaeozoic emplacement ages for migmatized granitic rocks sourced from granulitic metasediments (Manton *et al.* 1992, Hand *et al.* 1994b). In addition, U-Pb data from adjacent older granitic rocks indicates significant early Palaeozoic disturbance (Manton *et al.* 1992). These data, together with the observation that D_4 zones deform 940±20 Ma granites (Hand *et al.* 1994b) and are kinematically very similar to regional Palaeozoic structures in Prydz Bay 200 km to the north-east (Dirks & Hand 1995, Carson *et al.* 1995, Carson *et al.* 1996) suggest D_4 and D_5 are early Palaeozoic in age.

Metamorphic geology

Although metapelitic rocks constitute < 1% of the outcrop in the Amery area, this study focuses on them since they contain numerous reaction textures that are useful to constrain the metamorphic evolution of the region.

Trost Rocks

Trost Rocks is a remote outcrop 80 km to the north of Jetty Peninsula on the northern edge of Single Island, a large ice covered island in south-western Amery Ice Shelf (Fig. 1), and consist of a sequence of pelitic and semi-pelitic gneiss, with syn-tectonic felsic intrusions. The layering dips vertically and trends 020°, although the significance of this fabric is unclear because the outcrop is too limited and inaccessible to allow detailed structural observations. The metapelite has two principle bulk compositions: layered aluminous corundum-absent migmatite and a corundum-bearing Fe-rich association. Both of these associations lack quartz. Mineral and textural relationships are summarized in Table II.

Corundum-absent assemblages are characterized by the growth of multiple generations of spinel and the stability of sillimanite throughout the history. The textural development can be divided into four stages:

1) Prograde inclusions in peak garnet indicate the early stability of spinel-biotite and sillimanite.

2) M_1 Peak assemblage is defined by coarse (100–2000 mm) granoblastic sillimanite-garnet-spinel-K-spar. Leucocratic patches within the rock suggest the peak assemblage was also associated with a melt phase.

3) Fine grained (< 100 mm) reaction textures involve the consumption of garnet and K-spar to produce a secondary biotite-spinel association (Fig. 2a & b) which defines a strong fabric. Garnets are pulled apart within this fabric

Table I. Summary of the structural and metamorphic history of the eastern nPCM.

Age (Ma)	Event	Deformation	Intrusive Activity	Metamorphism
Early to Mid Proterozoic¥	Igneous and sedimentary protoliths			
			Mafic dykes†	
1020-980 Ma #‡¥	**D_{1-2}** D_1* D_{1-4}† MY1+	Formation of a regional gneissic layering	Voluminous felsic intrusions*¥	Granulite metamorphism P= 6-7 kbars, T= 750-830°C *†◊
c. 980-940 Ma ∞#	**D_3** D_2* D_5†	E-W folding with strain partitioning into large east-west shear zones with east plunging lineation.	Leucogneiss Garnet granite*	
c. 500 Ma?	**D_4** D_2* D_6† MY2+	Mylonitic high strain zones with SE-plunging lineations		Granulite metamorphism P = 4.5 kbars, T = 700 °C *◊
~500 Ma #	**D_5** D_3* D_8†	Approximately north trending shear zones with upright S_3 foliation.*	Granitic dykes.* Large pegmatite bodies and veins.*	Amphibolite facies metamorphism.*
	Uplift			
*c.*300 Ma§		North-south trending brittle faults.	Mafic dykes.	Hydrothermal alteration.
	Exposure of eastern nPCM at surface, Permo-Triassic sedimentation			
c. 140 Maß		Brittle faulting associated with development of Lambert Graben	Alkaline mafic and ultramafic dykes and stocks.	

◊ This study; * Jetty Peninsula, Hand et al (1994a,b); † Porthos and Aramis Ranges, Fitzsimons & Thost (1992); ‡ Tingey (1982); # Manton *et al.* (1992); § Hofmann (1991); ß Andronikov (1990); ∞ Scrimgeour (1994); + Nichols (1995); ¥ Kinny et al (1997).

and have developed fractures that contain new biotite and spinel. Locally this assemblage is overgrown by fine grained sillimanite that sometimes rims the secondary spinel (Fig. 2a). This sillimanite-bearing assemblage is best developed where it rims primary garnet. The observation that new sillimanite grew during this stage suggests the stable fabric assemblage was biotite-sillimanite-spinel ± K-spar.

4) The final stage of the textural development involved reaction of the metastable association of biotite-spinel-sillimanite-relic M_1 garnet to produce M_2 cordierite-K-spar symplectites and cordierite-spinel-K-spar symplectites(Fig. 2c–f). The cordierite-K-spar symplectites form preferentially between garnet and biotite whereas the cordierite-spinel-K-spar symplectites form adjacent to sillimanite (Fig. 2e). Locally, in reaction volumes away from sillimanite, small (50 mm) garnets grew in conjunction with cordierite and spinel (Fig. 2a & b).

The textural development in *corundum-bearing assemblages* is similar to that of the corundum-absent assemblages, with the exception that the peak assemblage does not contain sillimanite. The peak M_1 assemblage is defined by granoblastic garnet-spinel-corundum-K-spar and is overgrown by a fine grained biotite-spinel-sillimanite assemblage. Sillimanite is

Table II. Assemblages in metapelites from Trost Rocks.

Rock	garnet	spinel	biotite	sill	Kspar	plag	corund	ilm	cord	quartz
TR1, 3	PR_3	IPR_1	IR_1	-	P	R_2	-	I	-	
TR4	PR_3	IPR_{12}	IR_1	R_1	PR_2	R_2	P	IR_2	R_2	R_3
TR8	PR_3	IPR_{12}	IR_1	IPR_1	PR_2	PR_2	-	IR_2	R_2	
TR11	PR_3	IPR_{12}	IR_1	IPR_1	PR_2	P	-	IR_2	R_2	

P = inferred to be part of the peak M_1 assemblage.
I = inclusion within M_1 garnet and/or sillimanite.
R = reaction textures consuming M_1 assemblage
R_1 = part of assemblage postdating M_1, pre-peak M_2 (S4 biotite fabric)
R_2 = inferred to be part of peak M_2 assemblage (cordierite coronas and symplectites)
R_3 = assemblage postdating peak M_2 (garnet overgrowing cordierite coronas)

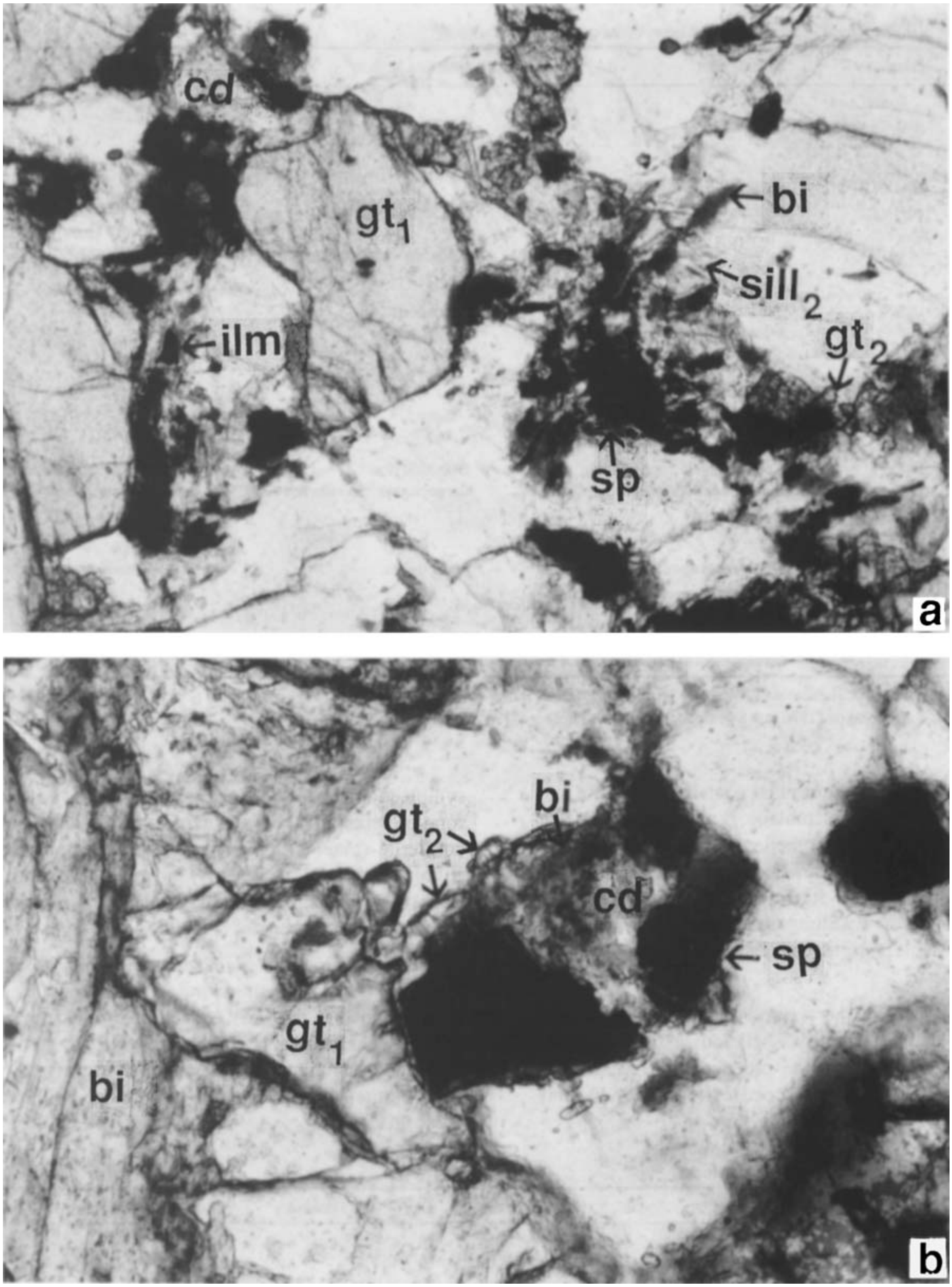

Fig. 2. Reaction textures in pelites from Trost Rocks. **a.** Garnet consumed by biotite and spinel, with sillimanite forming coronas around ilmenite and spinel, and fibres overgrowing biotite. Small late euhedral garnets also occur. Width of field of view is 2 mm. **b.** Primary garnet extensively consumed by biotite and spinel. Cordierite occurs partially consuming the biotite and spinel and all three minerals are overgrown by narrow coronas of secondary garnet. Width of field of view is 0.5 mm. **c.** Primary sillimanite consumed by biotite and by extremely fine grained symplectites of spinel and cordierite. Spinel is also overgrowing biotite. Width of field of view is 2 mm. **d.** Back scattered electron image showing a symplectite of cordierite and K-feldspar formed at the expense of primary garnet and biotite. Scale bar is 100 mm. Sample 964TR8.

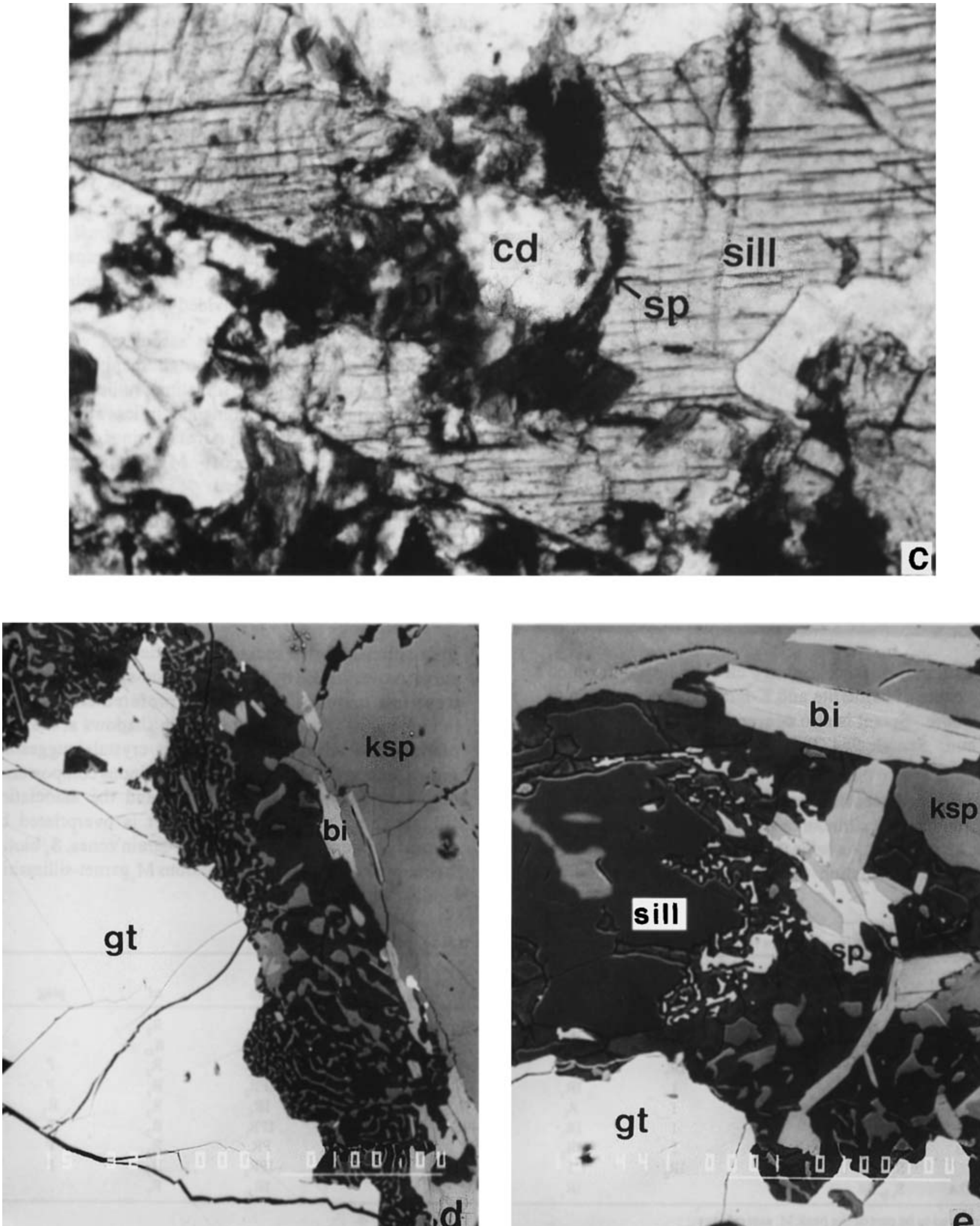

Fig. 2. (cont) **e.** Back scattered electron image in which cordierite separates biotite, sillimanite and garnet and contains vermicular intergrowths of spinel around sillimanite and K-feldspar around garnet adjacent to biotite. Note also the consumption of biotite by spinel. Scale bar is 100 mm. Sample 964TR8.

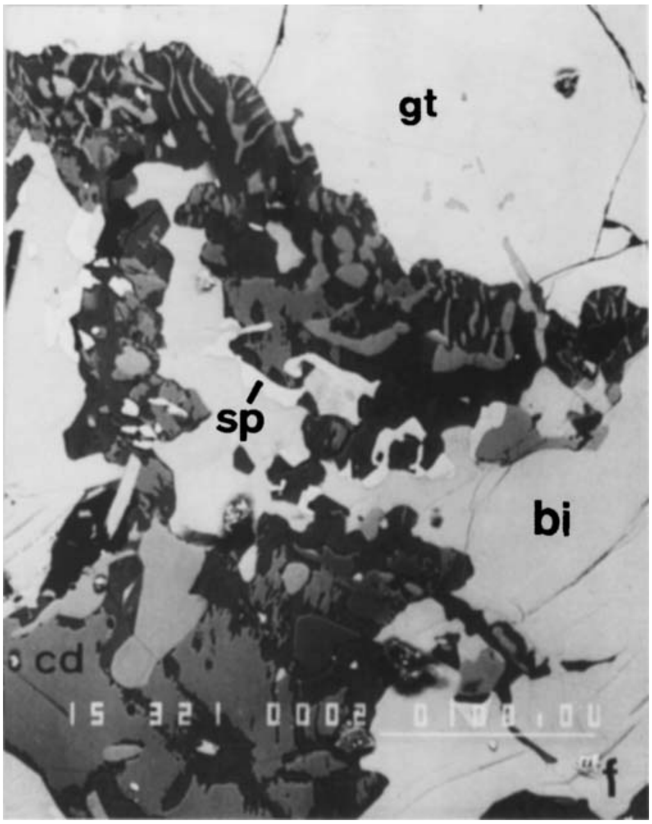

Fig. 2. (cont) **f.** Back scattered electron image in which a symplectite of cordierite and K-feldspar separates garnet and biotite. Spinel is also consuming biotite. Scale bar is 100 mm. Sample 964TR4.

never found adjacent to corundum, suggesting the association of corundum and sillimanite was not stable during the post-peak M_1 history. As with the corundum-absent rocks, the metastable association of biotite-sillimanite-spinel-relic garnet is overprinted by M_2 cordierite-spinel-K-spar symplectites.

Jetty Peninsula

The textural evolution of metapelitic rocks from Jetty Peninsula (Hand *et al.* 1994a) is summarized in Table III; these rocks form the closest related outcrop to Trost Rocks. Furthermore, unlike those at Trost Rocks, the metamorphic assemblages on Jetty Peninsula can be related to the regional structural framework and therefore provide a useful comparison. In quartz-sillimanite-bearing rocks on Jetty Peninsula, the textural development can be divided into four stages:

1) Migmatitic S_{1-2} layering is associated with an M_1 assemblage consisting of coarse sillimanite, commonly intergrown with ilmenite and sometimes rutile, that encloses garnet and quartz-K-spar domains. In less siliceous bulk compositions (e.g. 93583), quartz is a minor component of the M_1 assemblage and post- M_1 textures may have effectively been quartz-absent.

2) Locally a strong S_4 foliation defined by biotite and secondary sillimanite deforms S_{1-2}. Both primary garnet and sillimanite are boudinaged and are locally enclosed within coarse plates of biotite, which also fill the microboudin necks.

3) In sillimanite-rich rocks, sillimanite-S_4 biotite and S_{1-2} garnet is overprinted by an M_2 cordierite-spinel association. Reaction textures are located preferentially within microboudins (Fig. 3a) and in strain shadows at the ends of deformed sillimanite and garnet crystals suggesting growth during D_4. In slightly less aluminous compositions (e.g. 904554E), no spinel formed and the association sillimanite-S_4 biotite and M_1 garnet is overprinted by coronal cordierite (Fig. 3b). In low-strain zones, S_4 biotite is commonly absent and the anhydrous M_1 garnet-sillimanite

Table III. Assemblages in metapelites from Jetty Peninsula (all samples contain quartz and K-feldspar).

Rock	Structural description	gt	sp	bi	sill	ru	ilm	cd	plag
904567	S_{1-2}, S4	PR_3	IR_1	IR_1	IPR_{13}		IR_2	R_2	
904559	D4 shear	P	IR_{12}	IR_{12}	P		R_2	R_{23}	
93583	S_{1-2}	IPR_3	IR_2	I	P		IR_2	R_2	P
904554E	S_{1-2}, S4	P	I	IR_1	IP		IPR_2	R_2	P
904570B	D4 shear	P	I	R_1	P		IR_1	R_2	R_2
93552A	F3 hinge	P	I	IR_1	IPR_1		IPR_1	R_2	P
93552B	F3 hinge	P	I	IR_1	IP		PR_2	R_2	P
96441	S_{1-2}	P	IR_2	I	IP	I	IPR_2	R_2	P
904562A	S_{1-2}, S4	P		IR_1	P		IR_2	R_2	

P = inferred to be part of the peak M_1 assemblage
I = inclusion within M_1 garnet and/or sillimanite
R = reaction textures consuming M_1 assemblage
R_1 = part of assemblage postdating M_1, pre-peak M_2 (S_4 biotite fabric)
R_2 = inferred to be part of peak M_2 assemblage (cordierite coronas and symplectites)
R_3 = assemblage postdating peak M_2 (late shear zones, garnet overgrowing cordierite coronas)

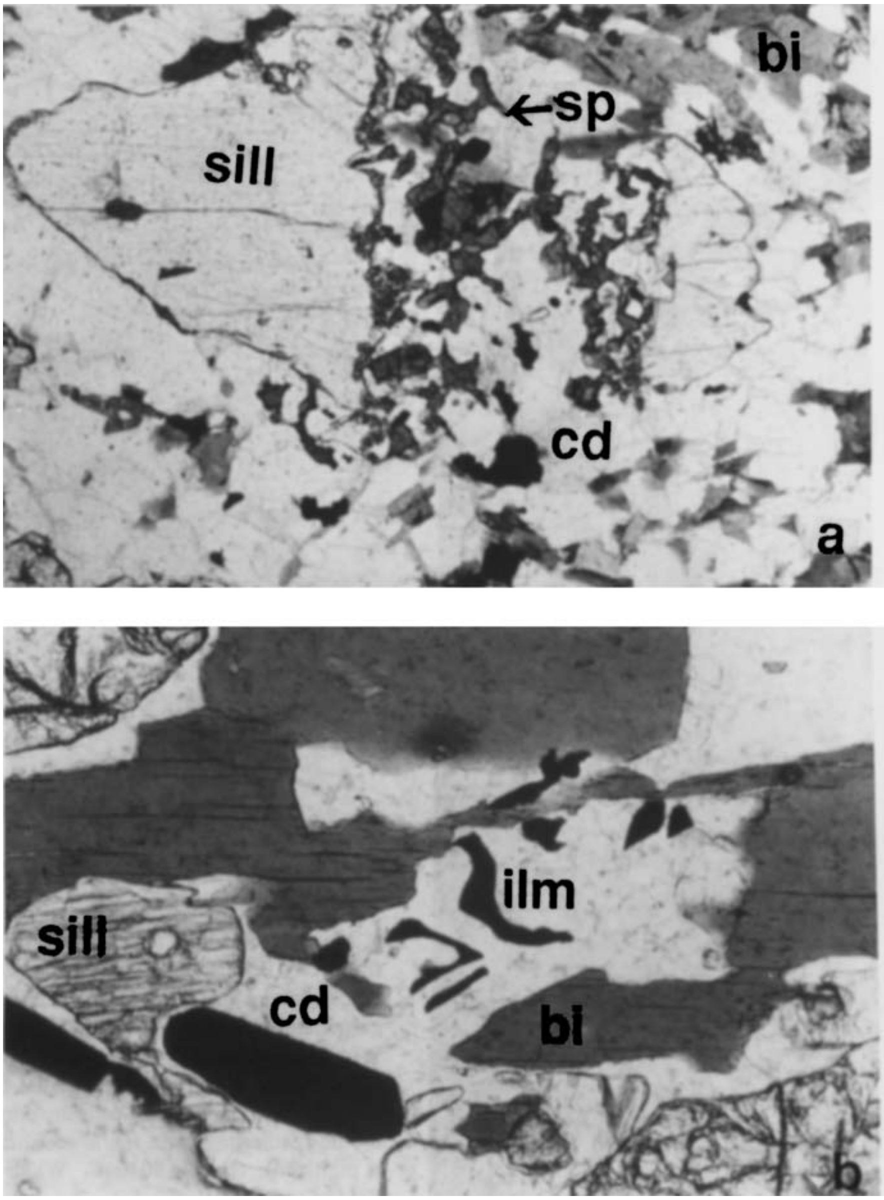

Fig. 3. Reaction textures in pelites from Jetty Peninsula. **a.** Intergrowth of spinel, cordierite and ilmenite replacing boudinaged sillimanite. Spinel is also overgrowing biotite. Width of field of view is 2 mm. **b.** Cordierite and ilmenite forming at the expense of biotite, sillimanite and garnet. Sample 904554E. Width of field of view is 2 mm.

association is overprinted by large cordierite coronas and cordierite-spinel symplectites (Fig. 3c).

4) Post-S_4 textures include the formation of a biotite-cordierite-quartz association. This is most pronounced in D_5 mylonite zones where biotite and recrystallized cordierite define the foliation and enclose porphyroblastic garnet and sillimanite (Fig. 3d). In low-strain domains, post S_4 textures include the formation of narrow sillimanite coronas on spinel and secondary garnet growth at the expense of cordierite.

Fox Ridge, Mcleod Massif

Fox Ridge is an E–W trending ridge on the western side of McLeod Massif, 40 km south-west of Jetty Peninsula (Fig. 1). It is dominated by a transitional granulite facies, east–west trending, high strain zone that dips steeply to the north and is reminiscent of the major D_4 shear zone on Jetty Peninsula (D_2 of Hand *et al.* 1994a). The similarity between the mylonite zones suggests they are probably associated with the same structural event (S. Boger personal communication 1997). The Fox Ridge metapelites preserve a complex textural record (Table IV) with the high strain fabric deforming and recrystallizing an earlier coarse grained M_1 assemblage which had been overprinted by low strain corona textures prior to mylonitisation. In the following description, these secondary assemblages will be referred to as $M_{2(F.R.)}$ so as not to directly imply an equivalence with M_2 at Trost Rocks and Jetty Peninsula.

In all samples of *pelitic gneiss* the peak M_1 assemblage

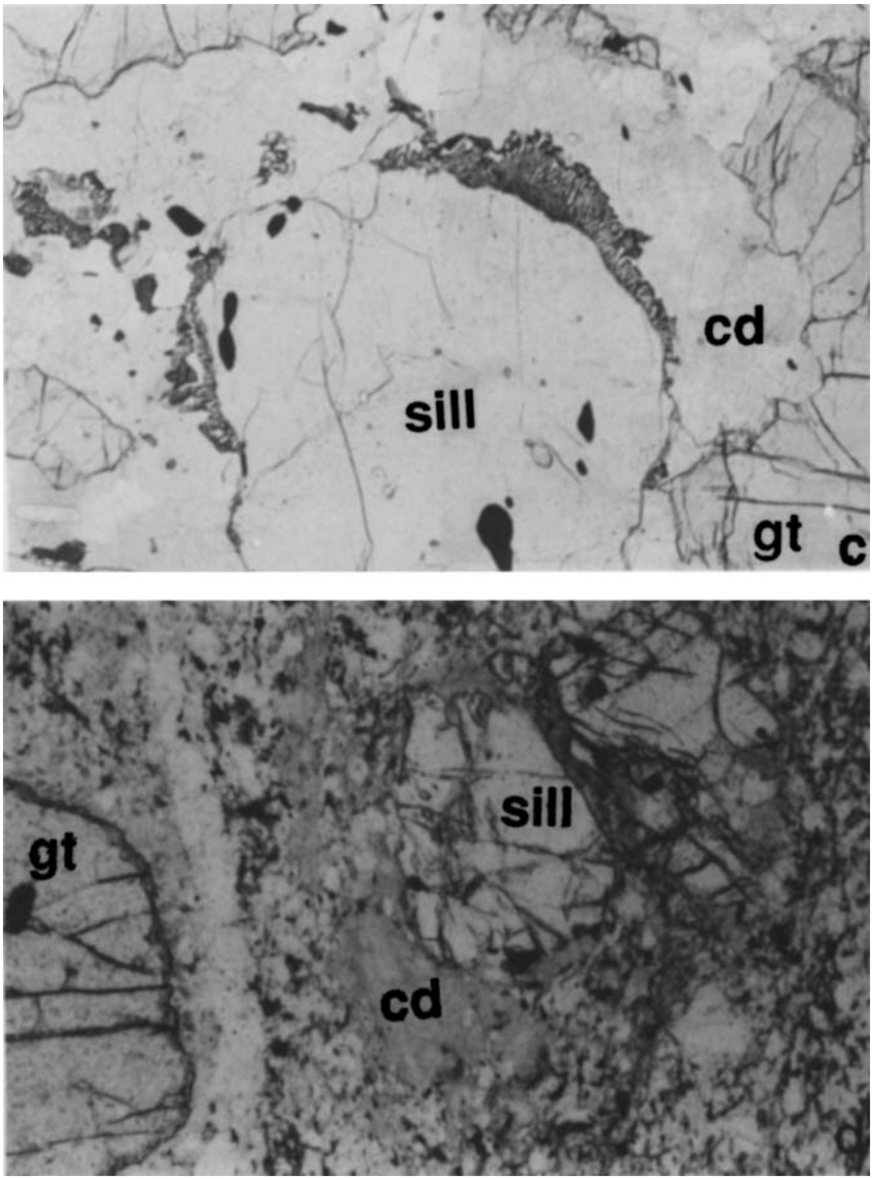

Fig. 3. (cont) Reaction textures in pelites from Jetty Peninsula. **c.** Symplectites of cordierite and spinel separating primary garnet and sillimanite. Sample 93583. Width of field of view is 3 mm. **d.** D_5 mylonite with porphyroblastic garnet and sillimanite enveloped and consumed by a biotite-cordierite-quartz fabric (cordierite is pinitized). Sample 90464C. Width of field of view is 2 mm.

contains garnet, usually with inclusions of sillimanite, quartz, spinel and less commonly biotite. Quartz, plagioclase and ilmenite are always present, and K-feldspar and rutile are common. Occurrences of rounded cordierite within garnet are also interpreted as primary inclusions, and in three samples (9645B, 96420C, 96424A), coarse porphyroblastic cordierite also forms part of the M_1 assemblage. In most samples, coarse blades of sillimanite, defining the S_{1-2} fabric occur both as inclusions within garnet and wrapping around large garnet porphyroblasts (Fig. 4a). Spinel commonly occurs as inclusions within the sillimanite, and corroded remnants of Zn-rich spinel within later cordierite are also interpreted to have grown during M_1. In slightly less aluminous and zincian assemblages (e.g. 9648C) spinel is absent, and the peak assemblage is interpreted to have been garnet-cordierite-quartz.

The M_1 assemblage is overgrown by $M_{2a(F.R.)}$ corona textures, which are dominated by cordierite, plagioclase and quartz. These textures enclose M_1 garnet porphyroblasts, and cordierite commonly separates garnet and sillimanite (Fig. 4b). Spinel inclusions in garnet are separated from the garnet by a moat of cordierite that is locally continuous with the coronas separating sillimanite and garnet.

The $M_{2a(F.R.)}$ cordierite coronas are deformed and recrystallized by a locally mylonitic high-strain fabric correlated with S_4 on Jetty Peninsula (S. Boger personal communication). In strongly mylonitized samples, the mylonitic assemblage is typically composed of garnet, plagioclase, quartz and ilmenite, with recrystallized cordierite. In almost all samples, small $M_{2b(F.R.)}$ garnets form trails that define the mylonitic fabric within recrystallized $M_{2a(F.R.)}$ cordierite (Fig. 4a & c). In a number of samples,

Table IV. Assemblages in lithologies from Fox Ridge (all samples contain quartz and plagioclase).

Rock	gt	sp	bi	sill	ru	ilm	cd	Kspar	corun	opx
4B, 4C	PR_3		IR_{34}			IR_3		PR_3		PR_3
5A	PR_3	I	R_4	IPR_4	P	IR_{34}	R_2R_3	PR_3		
5B	PR_3	I	IR_4	PR_4	I	IR_4	IPR_2	P		
8C	P		R_4	R_4	P	R_4	R_2R_3			
10A	PR_3	IPR_2	R_4	PR_4	I	IR_{23}	R_{23}	PR_3	P	
18A	PR_3	I	R_4	IPR_4		IR_4	R_{23}	P		
18B	PR_3	IP	R_4	PR_4	R_2	R_{23}	R_{23}	P		
19A	PR_3	I	R_4	IPR_4	I	R_{234}	R_2	P		
19B	PR_3	IR_2	R_4	PR_4		IR_{23}	R_{23}	P		
20B	PR_3	IP	R_4	R_4	IR_4	IR_4	R_{23}	PR_3		
20C	PR_3	P	R_4	R_4		IR_4	IPR_{23}	P		
23B	PR_3	I	I	IPR_4	I	IR_4	R_{23}	PR_3		
24A	PR_3	IP	R_4	IR_4	?	IR_4	PR_{23}	PR_3		

P = inferred to be part of the peak M_1 assemblage.
I = inclusion within M_1 garnet and/or sillimanite.
R = reaction textures consuming M_1 assemblage
R_2 = inferred to be part of peak M_2 assemblage ($M_{2a(F.R)}$ - cordierite coronas and symplectites)
R_3 = assemblage postdating peak M_2 ($M_{2b(F.R)}$ - mylonites recrystallizing cordierite coronas)
R_4 = late mylonite zones ($M_{2c(F.R)}$)

porphyroclastic sillimanite and garnet are pulled apart along the mylonitic fabric and these pull-aparts are filled by ilmenite and biotite. Ilmenite commonly forms vermicular intergrowths with secondary garnet, and garnet also forms coronas around trails of ilmenite defining the mylonitic fabric.

The $M_{2b(F.R.)}$ high strain fabric is reworked by a coplanar fine grained $M_{2c(F.R.)}$ biotite-sillimanite-ilmenite mylonitic fabric that envelopes $M_{2a(F.R.)}$ garnet and cordierite. In low strain domains biotite and fibrous sillimanite also form along the boundaries of cordierite and garnet. In sample 9648C porphyroclastic cordierite is substantially consumed by biotite and sillimanite, however cordierite is also recrystallized within the biotite-sillimanite fabric suggesting the association biotite-sillimanite-cordierite-quartz was stable toward the end of the $M_{2(F.R.)}$ metamorphic episode (Fig. 4d). The $M_{2c(F.R.)}$ assemblages are overprinted by biotite-ilmenite-quartz-bearing ultramylonites and essentially unoriented biotite and sillimanite.

In sample 9644B&C, *orthopyroxene-garnet felsic gneiss,* M_1 garnet-orthopyroxene-plagioclase-K-spar-quartz is overprinted by the S_4 mylonitic fabric. M_1 garnet growth appears to have outlasted orthopyroxene, with the latter commonly enclosed by garnet. An anastomosing S_4 shear fabric is defined by fine grained (20–30 mm) trails of $M_{2(F.R.)}$ garnet and orthopyroxene, associated with oriented biotite and dynamically recrystallized quartz and feldspar. Biotite often envelops the M_2 garnet and orthopyroxene, suggesting much of it formed relatively late during development of S_4.

Mineral chemistry

Mineral analyses were obtained at the Universities of Adelaide and Melbourne using a JEOL 733, and Cameca SX50 and 51 Camebax microprobes. Accelerating voltages of 20 kV were used on the JEOL 733 and 15 kV on the Cameca. A beam current of 20 nA was used on all instruments. Representative mineral compositions from Trost Rocks and Fox Ridge are shown in Table V. Analyses from Jetty Peninsula are given in Hand *et al.* (1994a).

Garnet

M_1 garnets are dominantly almandine-pyrope mixtures with X_{Fe} (Fe/Fe+Mn+Mg+Ca) ranging between 0.6–0.8 and X_{Mg} 0.2–0.35. X_{Ca} is generally less than 0.05. There is a consistent zoning in the garnets with X_{Fe} increasing by 0.05 to 0.1 units within 20 mm of the rims. The zoning is most pronounced toward contacts with cordierite and biotite, and can be attributed either to the growth of these relatively magnesian phases at the expense of garnet, or to retrograde Fe–Mg exchange during cooling. The cores of M_2 garnets have similar X_{Fe} to the rims of M_1 garnets and also show a rimward enrichment in Fe of 0.02–0.05 units. In felsic rocks, garnets show a rimward increase in X_{Ca} (0.055–> 0.07) toward contacts with plagioclase.

Cordierite

There is considerable compositional variation in cordierite. X_{Fe} (Fe/Fe+Mg) in M_1 cordierite from Fox Ridge ranges between 0.30–0.45 and shows a rimward decrease toward garnet of $\leq$ 0.05 units. $M_{2a(F.R.)}$ coronas at Fox Ridge are slightly less Fe-rich (0.02–0.04) than M_1 cordierite in the same sample. X_{Fe} in recrystallized cordierite defining the shear fabric on Fox Ridge is generally 0.03–0.05 units lower than M_1 cordierite, however there is considerable intrasample variation (up to 0.08 units). Cordierite within coronas and symplectites at Trost rocks is relatively constant in composition

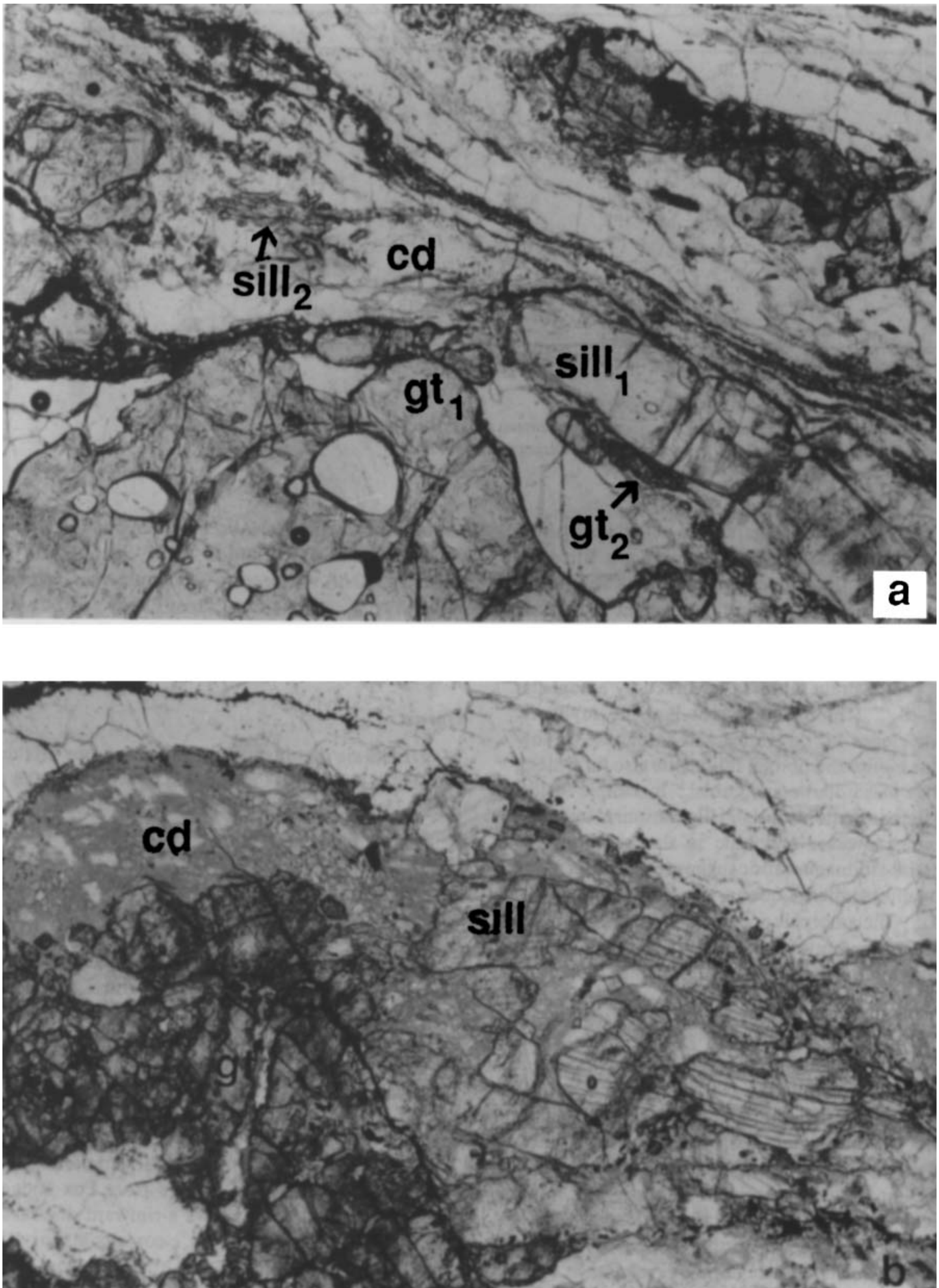

Fig. 4. Reaction textures in pelites from Fox Ridge. **a.** Porphyroblastic M_1 garnet and prismatic M_1 sillimanite separated by cordierite. M_2 garnet and fibrous sillimanite define a mylonitic fabric. Sample 9645A. Width of field of view is 2 mm. **b.** Corona of cordierite separating M_1 garnet and sillimanite. Sample 96410A. Width of field of view is 2 mm.

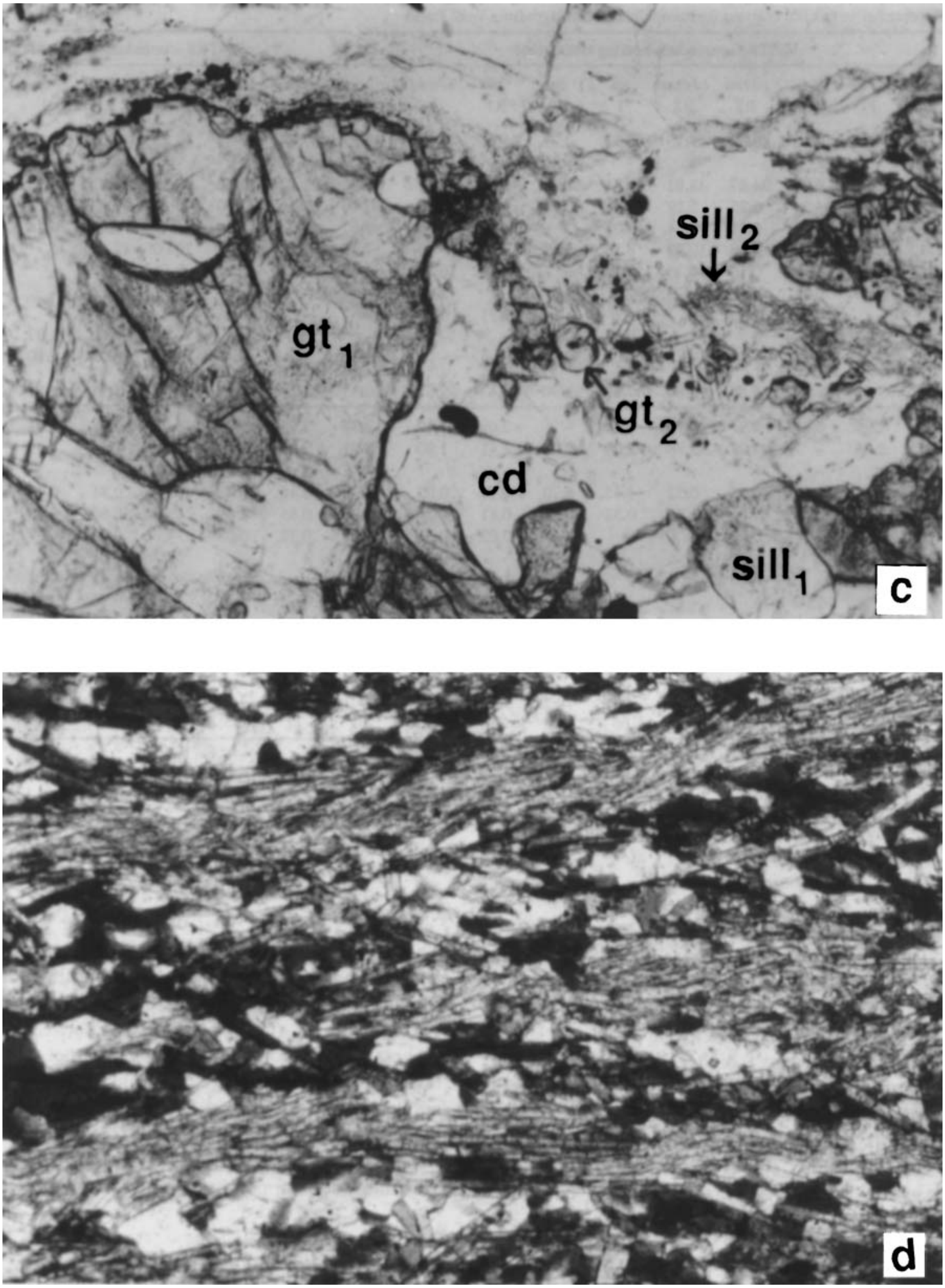

Fig. 4. (cont) Reaction textures in pelites from Fox Ridge. **c.** M_1 garnet and sillimanite consumed by cordierite, with secondary garnet and sillimanite occurring in the cordierite where it has been recrystallized in the mylonitic fabric. Sample 9645A. Width of field of view is 2 mm. **d.** M_{2c} biotite - sillimanite - cordierite assemblage. Sample 9648C. Width of field of view is 1 mm.

Table Va. Representative mineral analyses for metapelitic assemblages from Trost Rocks

	935TR4 - corundum-bearing assemblage									984TR8 - corundum-absent assemblage							
Mineral	gt rim	gt core	ilm	cd rim	cd core	sp	sp	bi	K-spar	gt core	gt rim	cd rim	cd	bi	sp	sp	plag
Texture*	P	P	R2	R2	R2	I	R2	R1	P	P	P	R2	R2	R1	I	R2	R2
SiO_2	38.27	37.92	0.12	49.30	49.15	0.32	0.23	35.95	47.52	37.82	37.97	49.32	49.73	35.65	0.21	0.37	54.35
TiO_2	-	-	52.71	-	-	-	-	6.86	0.11	-	–	-	-	6.40	-	-	-
Al_2O_3	22.61	22.21	0.06	34.07	33.81	62.34	62.39	15.97	33.17	21.96	22.32	33.60	34.10	16.42	60.83	61.76	28.45
FeO	31.23	28.72	44.35	5.35	5.19	28.45	30.34	14.09	0.45	30.70	33.16	5.60	5.11	14.52	31.14	30.77	0.49
MnO	0.85	0.55	0.30	0.01	0.14	0.05	-	–	–	0.67	1.04	-	-	0.31	0.16	0.21	0.07
MgO	6.31	8.11	1.13	9.98	10.27	8.18	6.23	12.73	–	7.75	5.64	9.74	10.00	12.61	6.77	7.19	–
CaO	1.48	1.69	–	0.16	0.28	0.16	-	0.16	16.33	1.49	1.41	0.26	0.15	0.24	–	–	10.58
Na_2O	–	0.02	0.11	-	-	-	-	-	2.03	–	–	–	-	-	-	-	5.57
K2O	-	-	0.03	-	-	-	-	9.71	0.01	–	–	–	-	9.74	-	-	0.07
Cr_2O_3	-	0.02	-	-	-	0.76	0.71	-	–	–	–	–	–	–	1.07	0.36	–
ZnO	–	–	–	0.03	-	0.03	0.06	–	–	-	-	-	-	0.02	0.10	0.16	-
Total	100.75	99.25	98.81	98.89	98.84	100.29	99.96	95.47	99.62	100.39	101.54	98.52	99.09	95.91	100.28	100.82	99.58
Si	2.98	2.96	0.01	4.97	4.98	–	-	2.69	2.19	2.94	2.95	5.00	4.97	2.68	0.01	0.01	2.46
Al	2.07	2.04	–	4.05	3.98	2.00	2.02	1.41	1.80	2.01	2.05	4.02	3.99	1.44	1.99	1.99	1.52
Fe_3	-	-	-	-	-	-	-	-	-	-	-	-	-	-	-	-	-
Fe_2	2.03	1.87	0.94	0.45	0.52	0.65	0.70	0.79	0.02	1.99	2.16	0.48	0.37	0.81	0.72	0.70	0.02
Mg	0.73	0.94	0.04	1.50	1.54	0.33	0.26	0.81	–	0.90	0.65	1.47	1.69	0.80	0.28	0.29	–
Ca	0.13	0.14	–	0.02	–	–	–	0.02	0.81	0.12	0.12	0.03	-	0.03	–	–	0.51
Na	–	–	–	-	–	-	-	-	0.18	–	–	–	0.02	-	-	-	0.49
K	–	–	–	–	–	–	–	1.41	-	–	–	–	–	1.41	-	-	-
Ti	–	–	1.00	–	–	–	–	0.39	–	–	–	–	–	0.36	-	-	–
Mn	0.06	0.04	-	–	–	–	–	–	–	0.04	0.07	–	–	–	–	0.01	–
Cr	–	–	–	–	–	0.01	0.01		–	–	–	–	–	–	0.02	0.01	–
Zn	–	–	–	–	–	-	-	–	–	0.01	–	–	–	–	–	–	–
Total	7.99	7.99	1.99	10.99	11.02	2.99	2.99	7.52	5.00	8.01	8.00	11.00	11.04	7.53	3.02	3.01	5.00
100XFe	74	67	96	23	25	66	73	49		69	77	25	18	50	72	71	

*Refer to Table II for textural abbreviation.

with X_{Fe} varying between 0.18–0.25.

Spinel

Spinel is hercynite-rich (X_{Fe} ($Fe^{2+}/Fe^{2+}+Mg+Mn+Zn$) = 0.65–0.85) with variable Zn and Cr. Magnetite contents are up to 3 mol%. At Fox Ridge, spinel inclusions in M_1 garnet generally have negligible Zn and Cr (< 0.02) and have a consistently higher X_{Fe} than the enclosing garnet. M_1 spinel from Trost Rocks also has a higher X_{Fe} than coexisting garnet. Corroded M_1 spinel enclosed in later cordierite from Fox Ridge contains appreciable X_{Zn} (up to 0.2) and X_{Cr} (Cr/Cr+Al) (up to 0.06). In contrast with M_1 compositional relationships, X_{Fe} in M_2 spinel is generally lower than coexisting garnet (by 0.02–0.05).

Biotite

In Fox Ridge metapelites X_{Fe} (Fe/Fe+Mg) in biotite ranges between 0.3–0.6, and within samples varies by up to 0.1. Ti contents are up to 0.3 per formula unit (p.f.u.) with higher Ti contents generally correlated with higher X_{Fe}. The compositional range of biotite at Trost Rocks is more restricted than at Fox Ridge with X_{Fe} ranging between 0.45–0.54 and Ti between 0.03–0.04 atoms p.f.u. In all instances biotite inclusions in M_1 garnet have lower X_{Fe} than M_2 biotite.

Feldspar

The orthoclase end-member in K-feldspar is typically 0.75–0.9 mol% and there is no appreciable difference between M_1 and M_2 K-spar. Plagioclase compositions are quite variable with X_{Ca} (Ca/Ca+Na) varying between 0.3–0.7, the highest anorthite contents occurring in garnet-orthopyroxene felsic gneiss on Fox Ridge. M_2 plagioclase associated with cordierite in the consumption of garnet generally has a higher anorthite content than M_1 plagioclase in the same sample, and mylonite plagioclase in felsic gneiss is also more anorthite-rich than porphyroclastic M_1 plagioclase.

Ilmenite

Mn and Mg contents are generally low (< 0.02 cations p.f.u.), and there is less than 3 mol% haematite solid solution.

Orthopyroxene

Porphyroclastic M_1 orthopyroxene in felsic mylonite shows a

Table Vb. Representative mineral analyses for metapelitic assemblages from Fox Ridge

	964-5B									96420C							
Mineral	gt rim	gt core	gt	cd rim	cd core	cd	cd	sp	bi	gt core	gt rim	gt	cd	cd	bi	plag	plag
Texture*	P	P	R3	P	P	R2	R3	I	R4	P	P	R3	R3	R2	R4	P	R2
SiO_2	37.66	37.34	37.11	47.31	46.99	47.46	46.75	0.17	34.51	37.50	37.44	36.80	47.99	48.69	36.98	55.85	49.44
TiO_2	-	-	-	-	0.04	-	-	-	3.52	0.05	–	0.18	0.15	0.25	5.25	0.15	0.23
Al_2O_3	21.99	22.27	22.17	32.60	32.49	32.50	32.27	56.56	18.40	22.05	21.99	21.65	33.06	33.36	15.54	27.58	32.33
FeO	34.04	33.94	34.82	8.01	8.51	7.40	8.44	32.28	19.31	32.59	32.97	34.02	6.69	5.59	14.30	0.16	0.11
MnO	1.17	0.93	0.95	0.20	0.20	-	0.10	0.09	0.10	0.82	0.88	1.11	0.05	-	-	0.10	0.14
MgO	4.39	5.02	4.14	8.04	7.94	8.67	8.52	3.69	8.99	5.53	5.32	4.05	9.29	9.83	14.03	-	0.13
CaO	1.36	1.30	1.36	0.11	-	0.03	-	0.11	0.32	1.51	1.62	1.54	0.13	0.07	0.07	9.98	15.09
Na_2O	–	-	-	0.03	0.06	-	0.04	-	-	-	–	-	-	-	-	5.92	2.87
K_2O	-	-	-	-	-	-	-	-	9.61	-	–	-	-	-	9.90	0.02	0.03
Cr_2O_3	-	-	-	-	-	-	-	1.31	-	–	–	–	-	–	–	-	-
ZnO	–	–	–	0.01	-	-	-	5.66	–	-		-	-	–	0.01	-	-
Total	100.61	100.80	100.55	96.31	96.23	96.06	96.14	99.87	94.76	100.05	100.22	99.35	97.36	97.79	96.08	99.78	100.38
Si	2.98	2.95	2.95	4.97	4.95	4.98	4.94	-	2.66	2.96	2.96	2.96	4.96	4.98	2.74	2.52	2.25
Al	2.05	2.07	2.08	4.04	4.04	4.02	4.02	1.91	1.67	2.05	2.05	2.05	4.02	4.02	1.36	1.47	1.74
Fe_3	-	-	-	-	-	-	-	0.05	-	-	-	-	-	-	-	-	-
Fe_2	2.25	2.24	2.31	0.70	0.75	0.65	0.75	0.72	1.24	2.15	2.18	2.29	0.58	0.48	0.89	0.01	-
Mg	0.52	0.59	0.49	1.26	1.25	1.36	1.34	0.16	1.03	0.65	0.63	0.49	1.43	1.50	1.55	-	0.01
Ca	0.12	0.11	0.12	0.01	-	–	–	-	0.03	0.13	0.14	0.13	0.01	0.01	0.01	0.48	0.74
Na	–	–	–	-	0.01	–	–	-	-	–	–	–	–	-	-	0.52	0.25
K	–	–	–	–	–	–	–	-	0.94	–	–	–	–	–	0.94	-	-
Ti	–	–	–	–	–	–	–	-	0.20	–	–	0.01	0.01	0.02	0.29	0.01	0.01
Mn	0.08	0.06	0.06	0.02	0.02	–	0.01	-	0.01	0.06	0.06	0.08	0.01	-	–	-	-
Cr	–	–	–	–	–	–	–	0.03	-	–	–	–	-	–	–	–	–
Zn	–	–	–	–	–	–	–	0.12	–	-	–	-	-	–	–	–	–
Total	7.99	8.02	8.00	11.01	11.01	11.01	11.05	2.99	7.78	8.00	8.01	8.00	11.02	11.00	7.76	5.00	5.00
100XFe	81	79	83	36	38	32	36	82	55	77	78	83	29	24	36		

*Refer to Table IV for textural abbreviation.

rimward decrease in X_{Fe} (Fe^{2+}/Fe^{2+}+Mg+Mn; 0.5–0.47) and X_{Al} (Al/Al+Si; 0.075–0.035). Secondary mylonitic orthopyroxene has a similar X_{Fe} and X_{Al} to the rims of porphyroclastic orthopyroxene.

Metamorphic evolution

The metamorphic history of the assemblages described above is considered in terms of reactions in the model system KFMASH (K_2O–FeO–MgO–Al_2O_3–SiO_2–H_2O). Although this system is a simplification of the chemical environment that accompanied metamorphism, numerous studies (e.g. Clarke *et al.* 1989, Hensen & Harley 1990, Xu *et al.* 1994, Fitzsimons 1996) have shown its general applicability to metapelitic systems. Given that leucosomes, interpreted as the products of partial melting are spatially associated with the mineral assemblages, the following discussion considers reactions between garnet(gt)-spinel(sp)-biotite(bi)-cordierite(crd)-sillimanite(sill)-K-feldspar(K-spar)-melt(l) ±quartz(qtz) and corundum(cor).

Figure 5 shows fluid-absent qualitative P–T grids applicable to the metamorphic assemblages observed in the Amery area and neighbouring Fox Ridge. Figure 5a is the grid developed by Clarke *et al.* (1989) and is applicable to both quartz-bearing and quartz-absent assemblages even though as noted by Clarke *et al.* (1989), the [opx] invariant point may be metastable with respect to H_2O-saturated equilibria (Grant 1985). Hensen & Harley (1990, fig. 2.17) presented an alternative topology to Fig. 5a where at low f_{O2} the [opx] invariant is not present, and the biotite-absent, spinel-absent and quartz-absent reactions casually cross in the low P–high T region of P–T space. Only at high f_{O2} where the stability field of spinel + quartz overlaps with the region of biotite melting is the [opx] invariant point created (Hensen & Harley 1990). In the discussion that follows, the relevant reactions in corundum-absent rocks are biotite-absent, spinel-absent and quartz-absent, and therefore it makes relatively little difference whether [opx] is considered to be stable or not.

Figure 5b shows a qualitative grid for corundum-bearing orthopyroxene-absent assemblages. Implicit in Fig. 5a & b is that cordierite is hydrous and can therefore occur as a reactant in melt-producing reactions. The stoichiometry of reactions in Fig. 5 depends on the Fe–Mg partitioning between phases, particularly garnet and spinel. Experimental and natural rock data indicate that garnet can be either more Fe-rich than spinel (e.g. Hensen 1972, Ellis *et al.* 1980, Clarke *et al.* 1989, Hand *et al.* 1994), or less Fe-rich (e.g. Clarke & Powell 1991, Sengupta *et al.* 1991, Fitzsimons 1996). However, some authors (e.g. Clarke *et al.* 1989, Waters 1991) have argued that Kd_{Fe-Mg} garnet-spinel is

Table Vc. Representative mineral analyses from garnet-opx mylonite, Fox Ridge

Mineral Texture*	plag P	gt rim P	opx rim P	opx core P	gt core P	kspar P	gt R3	opx R3	bi R3	plag R3
SiO_2	48.33	37.66	50.17	49.87	37.64	64.72	37.79	51.66	36.72	46.76
TiO_2	0.00	0.00	0.04	0.04	0.04	-	0.03	0.10	4.89	0.01
Al_2O_3	31.99	20.75	2.03	3.20	20.89	18.06	20.87	1.36	14.47	32.78
FeO	0.14	31.83	28.90	28.98	31.79	-	31.35	28.71	15.51	0.77
MnO	0.01	1.41	0.36	0.40	1.34	0.01	1.23	0.30	0.01	-
MgO	-	5.07	17.45	16.79	5.61	0.01	4.91	17.68	13.29	-
CaO	16.73	2.45	0.14	0.15	1.94	0.06	2.71	0.13	-	17.85
Na_2O	2.22	-	0.02	-	0.03	1.02	0.04	-	0.07	1.50
K_2O	0.05	-	-	-	-	15.22	-	0.04	10.07	0.02
Cr_2O_3	0.02	0.03	0.07	0.06	-	0.07	-	0.01	0.01	-
ZnO	-	0.13	0.04	-	-	0.08	0.04	0.18	-	0.08
Total	99.80	99.40	99.28	99.49	99.30	99.27	99.13	100.17	96.01	99.93
Si	2.22	3.01	1.94	1.93	3.00	3.00	3.02	1.98	5.49	2.16
Al	1.73	1.95	0.09	0.15	1.96	0.99	1.96	0.06	2.55	1.79
Fe_3	-	-	-	-	-	-	-	-	-	-
Fe_2	0.01	2.13	0.94	0.94	2.12	-	2.09	0.92	1.94	0.03
Mg	-	0.60	1.01	0.97	0.67	-	0.59	1.01	2.96	-
Ca	0.82	0.21	0.01	0.01	0.17	-	0.23	0.01	-	0.88
Na	0.20	-	-	-	0.01	0.09	0.01	-	0.02	0.13
K	-	-	-	-	-	0.90	-	-	1.92	-
Ti	-	0.10	-	-	0.09	-	0.08	-	0.55	-
Mn	-	0.02	0.01	0.01	-	-	0.04	0.01	-	-
Cr	-	-	-	-	-	-	-	-	-	-
Zn	-	0.01	-	-	-	-	-	0.01	-	-
Total	5.03	8.02	4.01	4.00	8.02	5.00	8.02	3.99	15.88	5.02
100XFe		78	48	49	76		78	48	40	

* Refer to Table IV for textural abbreviation

readily reset during cooling, with the result that measured compositions no longer reflect those at which the assemblages developed. An additional source of uncertainty in the Kd_{Fe-Mg} garnet-spinel comes from the estimate of Fe^{3+}. For example underestimating Fe^{3+} will lead to an overestimate of X_{Fe} spinel. Finally reactions involving Fe–Mg phases contain singularities (e.g. Hensen 1987, Nichols *et al.* 1995, Worley & Powell 1997) where the partitioning of Fe–Mg between coexisting phases inverts, meaning that a consistent partitioning does not occur across P–T space. The compositional data from the Amery area highlights some of these uncertainties. In Jetty Peninsula metapelites, X_{Fe} spinel < X_{Fe} garnet in the peak assemblage (Hand *et al.* 1994a), whereas the reverse is true for Trost Rocks and the inclusion assemblage in M_1 garnet on Fox Ridge. Furthermore, in the secondary fine grained assemblages at Trost Rocks, X_{Fe} spinel < X_{Fe} garnet. In the absence of conclusive evidence, the reactions in Figs 5 & 6 assume that X_{Fe} spinel < X_{Fe} garnet. This results in all reactions having positive PT slopes with melt on the high-T side. For the situation where X_{Fe} spinel > X_{Fe} garnet Fig. 5a & b would look slightly different, with both the cordierite-absent and biotite-absent reactions likely to have negative slopes so that melt occurs on the high-T side (e.g. Fitzsimons 1996).

Because mineral assemblages are dependant on bulk composition and are usually at least divariant, the interpretation of reaction textures using invariant grids alone can be misleading. For this reason pseudosections (Hensen 1971) are employed to assess the relative changes in P–T implied by the observed mineral reactions. Figs 5c–e & 6a–b show P–T pseudosections for bulk compositions appropriate to the metapelites in the Amery area and at Fox Ridge. Three broad bulk compositional groups exist:

1) quartz- and corundum-absent assemblages in which spinel appears to be stable at all times (Trost Rocks),
2) quartz-absent, corundum-bearing assemblages (Trost Rocks), and
3) quartz-bearing assemblages (Jetty Peninsula and Fox Ridge).

The pseudosections are constructed on the basis that garnet-sillimanite-cordierite-quartz and sillimanite-spinel-cordierite-quartz equilibria have relatively shallow slopes in PT space (Nichols *et al.* 1992, Hensen & Green 1971, Aranovich & Podlesskii 1983) and garnet-spinel-sillimanite-quartz and garnet-sillimanite-spinel-corundum have moderate P–T slopes (Bohlen *et al.* 1986). The widths of the fields are approximate only.

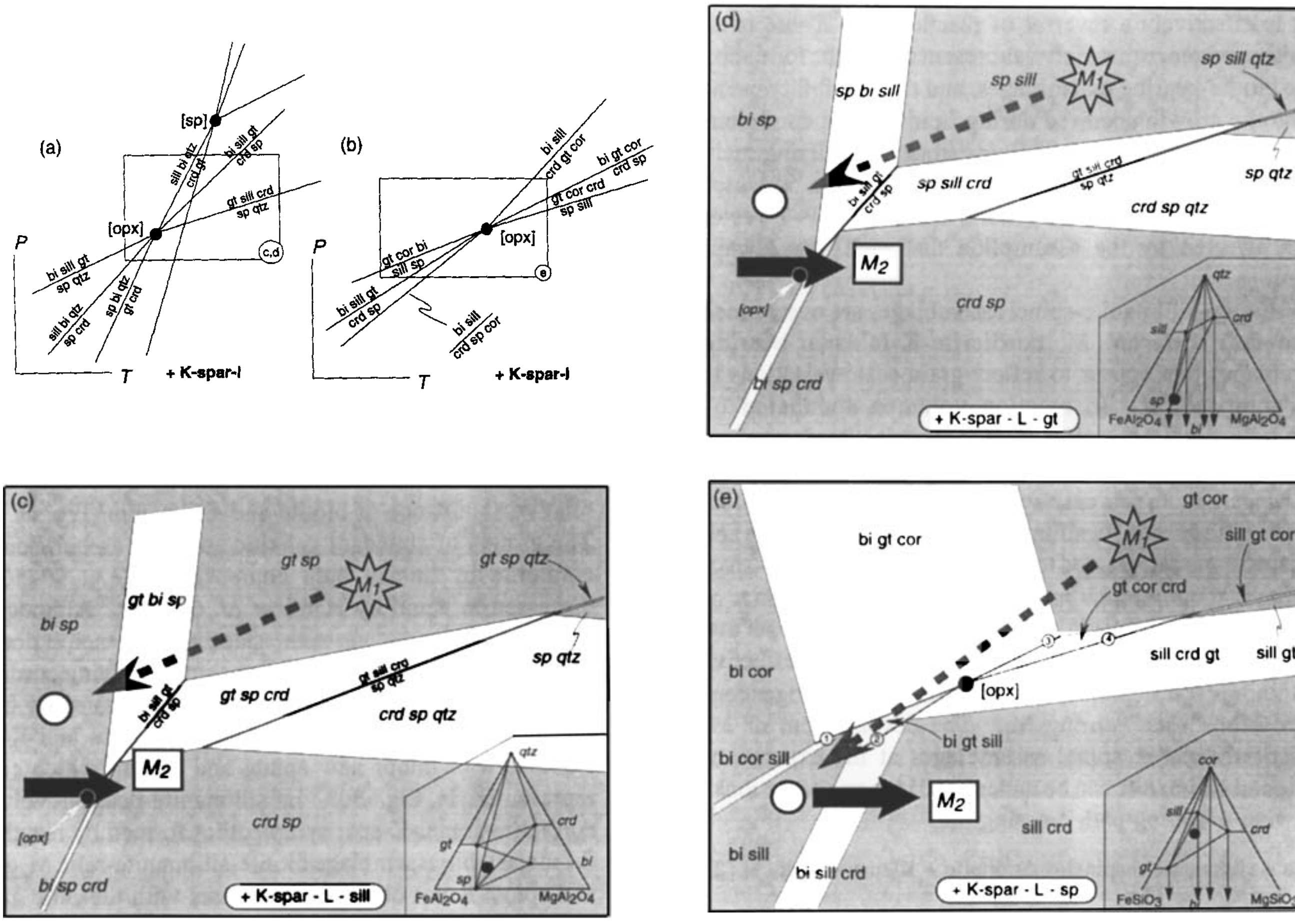

Fig. 5. Qualitative KFMASH equilibria for fluid-absent metapelites. The grids in **a** and **b** show univariant equilibria assuming X_{Fe} garnet > X_{Fe} spinel and form the basis of the P–T pseudosections in **c-e**. Stars represent the position of the peak M_1 assemblages, the open circles the biotite-sillimanite ± spinel-bearing post- M_1 assemblages and squares, peak M_2 cordierite-bearing assemblages. The dashed arrow shows the inferred M_1 retrograde path and the black arrow represents the inferred M_2 path. In **a.** the position of the invariant point is about 400 MPa and 740°C (Fitzsimons 1996), and in **b.** using THERMOCALC (Powell & Holland 1988, 1996 personal communication) is calculated to be at 510 MPa at 742°C for an aH_2O = 0.25. Boxes labelled **c-e** show the approximate positions of the pseudosections in **c-e**. **c.** Pseudosection for an aluminous bulk composition (black circle in inset) in which spinel and sillimanite are stable throughout the metamorphic evolution. Peak M_1 conditions are characterized by the stability of garnet-sillimanite-spinel and the absence of cordierite and biotite. Peak M_2 assemblages contain cordierite and spinel which formed at the expense of lower-T biotite assemblages. The presence of biotite-sillimanite-spinel-bearing assemblages between M_1 and M_2 implies cooling from M_1 prior to M_2 (dashed arrow). **d.** Pseudosection for a less aluminous Fe-rich composition, appropriate to the "effective" bulk composition during the development of M_2 assemblages in local volumes dominated by garnet. In both **c** and **d**, the growth of cordierite-bearing assemblages implies heating during M_2. **e.** In corundum-bearing assemblages, the peak association of garnet-spinel-corundum is overprinted by biotite-sillimanite-spinel prior to M_2 implying some exhumation accompanied cooling between M_1 and M_2. The subsequent growth of M_2 cordierite and K-spar implies heating. Reaction 1 = (cordierite absent), reaction 2 = (corundum absent), reaction 3 = (sillimanite absent), reaction 4 = (biotite absent), (from Fig. 5b).

Trost Rocks

Peak *corundum-absent assemblages* are characterized by the association of garnet-sillimanite-spinel, and the absence of cordierite and biotite. The presence of biotite-sillimanite-spinel-bearing inclusion assemblages in peak garnet suggests the divariant melting reaction,

spinel + biotite + sillimanite = garnet + K-spar + melt (1)

was crossed on the prograde path resulting in biotite-absent peak assemblages.

The appearance of biotite-bearing assemblages without cordierite, overprinting the peak M_1 assemblages is *consistent* with near-isobaric cooling from peak conditions (Fig. 5c). The most common retrograde texture is the breakdown of M_1 garnet and K-spar to produce a spinel-biotite association. Further cooling is suggested by the growth of new sillimanite to form a biotite-spinel-sillimanite association (Fig. 5c) in what is effectively a reversal of reaction (1). There is no definitive evidence that melt was present during the formation of the biotite-bearing assemblages, and the possibility exists that biotite growth occurred during fluid-present conditions resulting from the release of fluids from crystallizing melt. Although this strictly cannot be portrayed in Fig. 5c which assumes melt is present, the general sense of the P–T vector is not affected by the assumption that melt was always present.

The biotite-sillimanite-spinel assemblages are overprinted by several different M_2 cordierite-K-feldspar-bearing assemblages that appear to reflect grain scale variations in bulk composition. In reaction volumes dominated by sillimanite, cordierite-spinel-K-spar symplectites formed by reaction of the metastable assemblage biotite-sillimanite-relic M_1 garnet. In this case spinel is not observed in contact with the relic garnet. In sillimanite-poor regions, biotite and remnant M_1 garnet, reacted to form M_2 cordierite and K-spar, together with minor new spinel and garnet. The presence of both these assemblages in a single thin section suggests that equilibration volumes were small during M_2, with effective partitioning of bulk compositions from the more homogeneous composition "seen" during M_1. The development of M_2 cordierite-K-spar ± spinel assemblages at the expense of biotite and sillimanite can be understood in terms of the rocks following a heating path crossing the,

biotite + sillimanite + spinel = cordierite + K-spar + melt, (2)

and

biotite + garnet + spinel = cordierite + K-spar + melt (3)

divariant reactions as indicated in Figs 5c & d. Since there is little baric constraint, the M_2 P–T vector is drawn approximately horizontally.

In *corundum-bearing assemblages* (e.g. TR4) the peak M_1 assemblage is defined by garnet-spinel-corundum-K-spar. Garnet contains inclusions of biotite and spinel, and the absence of sillimanite as an included phase possibly suggests a near isobaric prograde path (Fig. 5e). The retrograde evolution resulted in the formation of fine grained biotite-spinel assemblages at the expense of garnet and K-spar and corundum. Continued reaction resulted in the growth of sillimanite which is never in contact with relic corundum and appears to have been stable with biotite and spinel. These reactions imply a cooling path with some decompression (Fig. 5e). Subsequent heating is implied by fine-grained M_2 cordierite-spinel-K-spar assemblages that developed between biotite and relic M_1 garnet (Fig. 5e).

Jetty Peninsula

Peak assemblages are characterized by the association of garnet-sillimanite-K-spar with variable amounts of quartz, and absence of cordierite and biotite. M_1 garnet contains inclusions of biotite-sillimanite-quartz ± (zincian-spinel) indicating the divariant melting reaction,

biotite + sillimanite + quartz = garnet + K-spar + melt, (4)

was crossed on the prograde path (Fig. 6a & b) resulting in biotite-absent peak assemblages.

As with Trost Rocks, the appearance of biotite-sillimanite-bearing assemblages without cordierite defining S_4 is consistent with a cooling path without significant decompression (Fig. 6a & b). The biotite-sillimanite assemblages are overprinted by several M_2 cordierite-bearing assemblages. In some assemblages (e.g. 904554E) M_2 cordierite coronas formed between biotite-sillimanite and relic garnet, resulting in the associations biotite-cordierite-garnet and sillimanite-cordierite-garnet, depending on the relative abundance of biotite and sillimanite (Fig. 6a & b). The growth of abundant gahnitic spinel in association with cordierite in zincian bulk compositions (e.g. 904567) is discussed in detail by Hand *et al.* (1994a). Although the presence of zinc increases the stability of spinel, it does not alter the essential textural relationships involving cordierite. Local quartz-absent reaction volumes dominated by biotite and remnant M_1 garnet formed M_2 cordierite and K-spar, together with minor new spinel and garnet, which can be represented in Fig. 5d. In sillimanite-bearing volumes, cordierite-spinel-K-spar symplectites formed by reaction of the metastable assemblage biotite-sillimanite-relic M_1 garnet and spinel is not observed in contact with the relic garnet. The development of M_2 cordierite-K-spar ± spinel or quartz assemblages at the expense of biotite-sillimanite-bearing assemblages can be understood in terms of the rocks following a heating path crossing reaction (2) and,

biotite + sillimanite + quartz = cordierite + K-spar + melt (5)

divariant reactions as indicated in Figs 5d, 6b & c. The final assemblage is associated with D_5 shear zones. In quartz-bearing rocks, S_5 is defined by biotite-cordierite-quartz, implying cooling with some decompression from peak- M_2 conditions (Fig. 6b).

Biotite-absent assemblages. Since the growth of retrograde biotite depends on local fluid pathways, some rock volumes will remain essentially biotite-absent. In these rocks (e.g. 93583, 96441, 904562A) there is no evidence for the post-M_1 near isobaric cooling path. During subsequent M_2 heating, M_1 garnet and sillimanite reacted directly to form cordierite-spinel-bearing assemblages essentially identical to those found in the biotite-bearing rocks, *implying* a decompressional P–T path that is *not* real (Fig. 6a & b).

Fox Ridge

Although the gneiss at Fox Ridge has been deformed by a high-strain mylonitic fabric, the presence of microboudins and low-strain domains preserving pre-mylonitic mineral

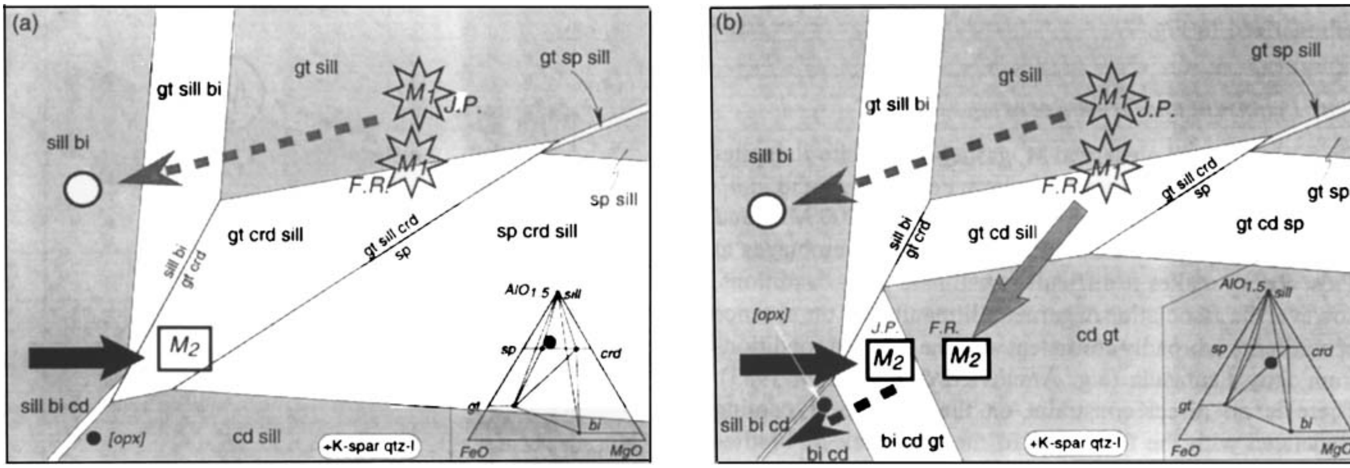

Fig. 6. Qualitative KFMASH P–T pseudosections for quartz-bearing bulk compositions appropriate to metapelites at Jetty Peninsula and Fox Ridge. The labelling scheme of assemblages and P–T vectors is the same as Fig. 5. **a.** Pseudosection for an aluminous bulk composition. Peak M_1 conditions on Jetty Peninsula ($M_{1\ J.P.}$) are characterized by the stability of garnet and sillimanite without cordierite and biotite, *implying* slightly higher pressures than the cordierite-bearing M_1 assemblages at Fox Ridge ($M_{2(F.R.)}$). At Jetty Peninsula, peak M_2 assemblages ($M_{2\ J.P.}$) contain cordierite which formed at the expense of lower-T biotite-sillimanite assemblages. Biotite is the least abundant M_2 reactant and is lost from the assemblage during M_2 heating, resulting in cordierite-sillimanite-garnet. **b.** Pseudosection for a less aluminous bulk composition (ie one with relatively little sillimanite). At Jetty Peninsula, the peak M_2 assemblage is M_2 cordierite-biotite-garnet, whereas at Fox Ridge, the initial mylonitic M_2 assemblage was garnet-cordierite-quartz ($M_{2\ F.R.}$). The black dashed arrow shows the post-peak M_2 path implied by the formation of D_5 biotite-cordierite-quartz assemblages. In **b** the shaded arrow represents the path implied by the cordierite-bearing coronas and mylonitic assemblages at Fox Ridge. Note also that in biotite-absent rocks from Jetty Peninsula (e.g. 93583) a decompressional path is *implied* by the formation of M_2 cordierite-bearing symplectites and coronas, however this path is misleading in terms of the evolutionary history of the Jetty Peninsula rocks. It should be noted that the implied difference in peak- M_1 and M_2 conditions between Fox Ridge and Jetty Peninsula could simply result from assemblages in slightly different bulk compositions being portrayed on the same pseudosections. The thermobarometric results suggest there is little difference in the peak- M_1 and M_2 conditions in both areas.

textures permits an evaluation of P–T evolution of these rocks.

The earliest identifiable assemblage is sillimanite-biotite-quartz-spinel which occurs as inclusions in M_1 garnet. This assemblage, and the presence of cordierite inclusions in some garnets (Table IV) is consistent with a broadly compressional prograde path (Fig. 6b) resulting in progressive loss of biotite from the assemblage and the formation of the peak association garnet-sillimanite-K-spar-quartz ± (cordierite and Zn-rich spinel). The peak M_1 assemblage was overprinted by cordierite coronas which separate garnet and sillimanite and isolate spinel inclusions from their garnet host. Assuming quartz, K-feldspar, and a melt phase were within the effective equilibration volume, the growth of $M_{2(F.R.)}$ cordierite at the expense of garnet and sillimanite indicates progress of the divariant reaction,

garnet+sillimanite+quartz=cordierite(+quartz-K-feldspar-melt) (6)

(Fig. 6). $M_{2(F.R.)}$ cordierite also forms at the expense of garnet and zincian spinel, implying progress of the higher-T reaction

garnet + spinel + quartz = cordierite, (+quartz-K-feldspar-melt) (7)

(Fig. 6b). However the reactive spinel in the Fox Ridge samples contains appreciable Zn which would have resulted in enlargement of spinel-bearing fields to lower temperatures. As a result, the formation of $M_{2(F.R.)}$ cordierite by reactions (6) and (7) may have occurred at the same temperature, rather than over a range of temperatures as implied by the Zn-absent equilibria in Fig. 6b.

The cordierite coronas have been deformed and recrystallized by a garnet-bearing high-strain fabric. Sillimanite is generally porphyroclastic in the fabric suggesting the stable assemblage was garnet-cordierite-quartz, implying the high strain fabric formed at temperatures similar to those that stabilized the pre-mylonitic cordierite coronas (Fig. 6b). A secondary mylonitic fabric defined in part by biotite and sillimanite together with finely recrystallized cordierite and quartz implies mylonitic deformation continued during slightly decompressive cooling (Fig. 6b).

Thermobaromerty

The high-T nature of the assemblages and in many cases, extensive M_2 re-equilibration resulting in the formation of high variance assemblages, makes it difficult to constrain

P–T conditions. The results of P–T calculations are summarized in Fig. 7.

Jetty Peninsula and Trost Rocks

On relatively well preserved M_1 garnet-sillimanite-ilmenite-rutile-quartz assemblages from Jetty Peninsula, Hand *et al.* (1994a) estimated peak M_1 conditions to be ~700 MPa and 800°C. The high variance of the peak M_1 assemblages at Trost Rocks makes it difficult to estimate peak conditions, however the association of garnet-sillimanite and the absence of cordierite is broadly consistent with the inferred conditions from Jetty Peninsula (e.g. Aranovich & Podlesskii 1983). There is no direct constraint on the amount of cooling associated with the formation of the post-peak M_1 biotite-sillimanite-bearing assemblages. However the degree of hydration associated with these assemblages suggests substantial melt crystallization (e.g. Fitzsimons 1996). If it is assumed the water saturated solidus was approached, or even crossed on a near-isobaric cooling path from peak M_1 conditions, the biotite-sillimanite ± spinel overprint may have formed at temperatures less than 700°C (e.g. Clemens & Wall 1981). Subsequent heating resulted in the growth of cordierite by crossing reactions 2, 3 and 5. Results of average pressure-temperature calculations using THERMOCALC (Powell & Holland 1988 1994) and the compositions of spinel-biotite-cordierite-K-spar-sillimanite with either quartz or spinel, suggests these divariant reactions were crossed at conditions around 450 ± 100 MPa and 700 ± 30°C. Since the divariant assemblage involves both cordierite and biotite, the results are sensitive to aH_2O, with both pressure and temperature increasing slightly with increasing aH_2O. Different calibrations of the GASP barometer (Newton & Haselton 1981, Hodges & Crowley 1985, Ganguly & Saxena 1984) on the M_2 assemblage garnet rim-plagioclase rim-sillimanite-quartz in samples 904554E and 904567 give results in the range 450–520 MPa at 725°C. In the same assemblages, M_1 garnet shows a pronounced increase in X_{Fe} toward contacts with M_2 cordierite. Assuming local equilibrium between M_1 garnet and M_2 cordierite rims, garnet-cordierite thermometry gives temperatures in the range 690–745°C at 450 MPa (Thompson 1976, Holdaway & Lee 1977, Bhattacharya *et al.* 1988).

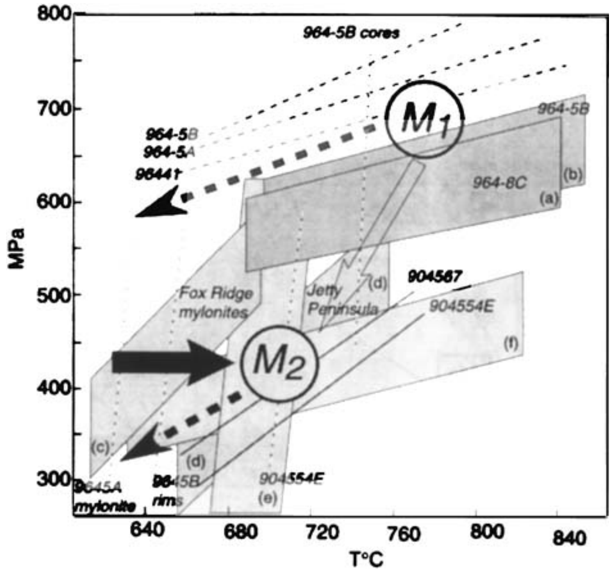

Fig. 7. Thermobarometric results from the Amery area and Fox Ridge. The fields labelled 'a' and 'b' are 1s envelopes for average-P calculations (Powell & Holland 1988, 1994) on the peak M_1 assemblage garnet-sillimanite-cordierite-ilmenite-rutile-quartz (aH_2O = 0.4) from Fox Ridge. The dashed lines show the results of applying the GRAIL calibration of Bohlen *et al.*, (1983a) to Fox Ridge and Jetty Peninsula peak M_1 assemblages. Dotted lines show the average of Fe–Mg garnet-cordierite thermometry (Thompson 1976, Holdaway & Lee 1977, Bhattacharya *et al.* 1988) for both M_1 and M_2 assemblages. The spread about the average is approximately ± 30°C. Solid lines show the average (± approximately 70 MPa) of several different GASP calibrations (Newton & Haselton 1981, Ganguly & Saxena 1984, Hodges & Crawley 1985, Holland & Powell personal communication 1995). Fields 'c' and 'd' are 1s envelopes for average-T calculations (Powell & Holland 1988, 1994) on the M_2 assemblage cordierite-sillimanite-biotite-K-spar-quartz from Jetty Peninsula and late stage mylonites from Fox Ridge. Fields 'e' and 'f' are the results of garnet-orthopyroxene-plagioclase-quartz thermobarometers using compositions in D_4 mylonitic felsic gneiss from Fox Ridge (Newton & Perkins 1981, Harley 1984, Essene 1989, Holland & Powell personal communication 1995, Bohlen *et al.* 1983b, Bhattacharya *et al.* 1991, Perkins & Chipera 1985, Lal 1993, Lee & Ganguly 1988). The P–T vectors are taken from Figs 5 & 6, with the open arrow indicating the *apparent* P–T path implied by the formation of the M_2 assemblages in biotite-absent rocks.

Fox Ridge

The extent of mylonitic reworking of M_1 assemblages on Fox Ridge makes it difficult to find well-preserved M_1 assemblages. The best examples of peak M_1 assemblages are in 964-5B and 964-8A. Calculations using the core composition of M_1 garnet and plagioclase, together with ilmenite, rutile, sillimanite and quartz and the GRAIL calibration of Bohlen *et al.* (1983a) and the thermodynamic dataset of Holland & Powell (1995 personal communication) gives pressures in the range 650–800 MPa over the interval 700–800°C. For the same assemblage (but including cordierite), and assuming a temperature of 750°C, average pressure calculations (Powell & Holland 1988, 1994) give results in the range 580±40 to 620±40 MPa for aH_2O = 0.4–0.6. Average-T calculations (Powell & Holland 1988, 1994) yield 740±50°C assuming a pressure of 600 MPa and aH_2O = 0.4. Fe–Mg exchange thermometry using core compositions of M_1 cordierite and garnet gives temperatures in the range 700–760°C at 650–750 MPa (Thompson 1976, Holdaway & Lee 1977, Bhattacharya *et al.* 1988).

The relatively high grade and fine grain size of the $M_{2(F.R.)}$ mylonitic assemblages means that Fe–Mg exchange thermometers will be unlikely to give near-peak $M_{2(F.R.)}$ temperatures (e.g. Frost & Jacko 1989). This is reflected by the results of garnet-cordierite and garnet-orthopyroxene thermometry on the mylonitic $M_{2(F.R.)}$ assemblages which give temperatures in the range 520–650°C for P = 400–500 MPa (Thompson 1976, Holdaway & Lee 1977, Bhattacharya *et al* 1988, Harley 1984, Lee & Ganguly 1988, Bhattacharya *et al* 1991, Lal 1993). Based on general petrological arguments, these results are probably some 50–80°C below peak $M_{2(F.R.)}$ conditions (e.g Harte & Hudson 1979, Pattison & Harte 1985). Slightly higher temperatures (630–700°C at 400–500 MPa) are obtained from garnet-rim, $M_{2a(F.R.)}$ cordierite corona compositions from local domains that escaped mylonitization. Barometric calculations using Fe-end member reactions in the mylonitic garnet-orthopyroxene-plagioclase-quartz assemblage in 964-4B give pressures in the range 360–400 MPa for a reference temperature of 650°C (Lal 1993, Essene 1989, Holland & Powell personal communication 1995, Bohlen *et al.* 1983b, Bhattacharya *et al.* 1991, Perkins & Chipera 1985). Similar pressures are obtained from compositions of porphyroclastic M_1 garnet-orthopyroxene-plagioclase from the same sample, reflecting the extent of re-equilibration of M_1 compositions in high strain domains during D_4. The final $M_{2(F.R.)}$ assemblage is the late-stage mylonitic biotite-sillimanite-quartz ± K-spar association. Average temperature calculations (Powell & Holland 1988, 1994) for this assemblage give 650±35°C at a pressure of 450 MPa. Although the extent of reworking of M_1 assemblages by the later mylonitic assemblages is significant in many cases, the general results of the thermobarometry are consistent with the relative sense of change between M_1 and peak M_2 conditions derived from Fig. 6.

Discussion and conclusions

The metapelitic assemblages in the eastern part of the Amery area show evidence for a complex metamorphic evolution with the stabilisation of relatively low-T biotite-sillimanite ± spinel-bearing assemblages in the interval between two thermal peaks recorded by M_1 and M_2 peak assemblages. The conclusion the rocks underwent a period of cooling from peak M_1 conditions is consistent with textures in interlayered calc-silicates from Jetty Peninsula. In the calc-silicates the formation of anorthite-calcite symplectites after scapolite, grossular ± quartz coronas between scapolite and wollastonite, and calcite-quartz symplectites replacing wollastonite (Hand *et al.* 1994b, Scrimgeour 1994) all suggest cooling in the vicinity of 800°C at around 700 MPa (i.e. peak M_1 conditions). Similar reaction textures have been described from the Nemesis Glacier region in the nPCM 60 km to the south-west (Fitzsimons & Harley 1994a) and have been attributed to near-isobaric cooling from ~800 to 700°C at *c.* 600 MPa. The fact the calc-silicates from Jetty Peninsula preserve a succession of reaction textures implying cooling, suggests they formed during continuous near-isobaric cooling from peak M_1 conditions, a conclusion consistent with the sequence of biotite and sillimanite-forming reactions from Trost Rocks. Subsequent heating at lower pressure conditions produced the cordierite-bearing peak M_2 assemblages without apparently reaching temperatures necessary to completely erase the cooling-style textures in the calc-silicates and metapelites.

Owing to the paucity of reactive assemblages in the nPCM (e.g. Fitzsimons & Thost 1992), the extent of the M_2 overprint is difficult to gauge. In the Fox Ridge metapelites, the development of secondary cordierite-bearing mylonitic assemblages at the expense of the M_1 garnet-sillimanite association, implies lower-P conditions, a conclusion supported by thermobarometry. A similar P–T evolution has been reported from the Mount Lanyon region 60 km south-west of Fox Ridge (Fig. 1) where mylonites overprinting the peak assemblages (600 MPa, 800°C) formed at *c.* 300 MPa and 700°C (Nichols 1995). This lower-P overprint is at odds with the near-isobaric cooling paths in the bulk of the nPCM immediately to the west (Fig. 8) (Fitzsimons & Thost 1992, Fitzsimons & Harley 1994a, 1994b, Thost & Hensen 1992, Nichols 1995, Scrimgeour unpublished data). Although there is no evidence the peak assemblages at Fox Ridge or Mount Lanyon initially followed an isobaric cooling path after M_1 (in contrast to the Amery area), the fact the lower-P overprint occurred at about the same pressure, and was associated with mylonitic deformation in all three areas, suggests it is reasonable to correlate the event across the entire region, an areal extent of ~12 000 km².

Hand *et al.* (1994a) offered two alternative models to account for observed mineral textures in the Amery area. One model suggested the textural evolution of the rocks reflected a broadly decompressional history during which temperatures fluctuated significantly. An important implication of this suggestion is that mid-crustal granulite events maybe short-lived compared to the duration of vertical movements in the crust. A second model suggested the Amery area had undergone two unrelated high-grade events, one at *c.* 1000 Ma (M_1) and the other (M_2), a lower pressure and temperature event at *c.* 500 Ma. Although Hand *et al.* (1994a) did not discount either model, they favoured the former on the basis that it was more consistent with the existing geochronological framework for region. However, recent recognition of the magnitude of Pan African reworking of Meso-Neoproterozoic granulites in Prydz Bay 200 km NE of the Amery area (Zhao *et al.* 1992, Hensen & Zhou 1995, Carson *et al.* 1996, Hand & Kinny 1996, Fitzsimons 1996, Fitzsimons *et al.* 1997) suggests a revaluation of this conclusion is warranted (e.g. Carson *et al.* 1996).

To the west of the Amery area, SHRIMP U-Pb geochronology by Kinny *et al.* (1997) has established that regional felsic magmatism in the nPCM occurred between 1020–980 Ma (Fig. 8) and was accompanied by granulite facies metamorphism, local partial melting and formation of minor leucogneiss bodies. The zircon populations analysed by Kinny *et al.* (1997) are all essentially concordant and show no evidence of post-980 Ma disturbance. Although it has yet to be conclusively demonstrated, it is assumed (e.g. Fitzsimons & Thost 1992, Thost & Hensen 1992, Fitzsimons & Harley 1994a, 1994b, Nichols 1995) that the isobaric cooling paths are associated with cooling from peak 1000 Ma conditions, rather than pseudo-cooling resulting from the superposition of a later, lower-T overprint (e.g. Hand *et al.* 1992). Indeed, *c.* 1000 Ma isobaric cooling seems reasonable given the volume of charnockitic magmatism late in the 1000 Ma event in the nPCM and adjacent regions (Fitzsimons & Thost 1992, Young & Black 1991).

The apparent simplicity of the U-Pb data from the nPCM contrasts with that from Jetty Peninsula, which also underwent granulite facies metamorphism and magmatism in the interval 1000–940 Ma (Manton *et al.* 1992). However, in contrast to the nPCM, new zircon and monazite growth occurred at *c.* 530 Ma in migmatized assemblages (Fig. 8), and Precambrian U-Pb systems were substantially disturbed in the early Palaeozoic (Manton *et al.* 1992). This isotopic picture is strongly reminiscent of results from Prydz Bay (e.g. Kinny *et al.* 1993) prior to the recent work that has conclusively demonstrated the magnitude of early Palaeozoic metamorphism in that region (Zhao *et al.* 1992, 1995, Carson *et al.* 1996, Hensen & Zhou 1995, Hand & Kinny 1996, Fitzsimons 1996, Fitzsimons *et al.* 1997). Since the M_2 reaction textures on Jetty Peninsula are associated with the youngest high-grade event in the region, and formed during prograde metamorphism, the strong implication is that M_2 reflects early Palaeozoic reworking of the *c.* 1000 Ma terrain. A similar re-interpretation of the metamorphic data of Hand *et al.* (1994a) was suggested by Carson *et al.* (1996). The Amery area therefore appears to occupy a transitional zone between the dominantly Proterozoic nPCM to the west, and the early Palaeozoic granulite belt in Prydz Bay to the north-east.

Evidence for possible additional complexity to the thermal history of the nPCM is provided by Hensen *et al.* (in press), who recognized a thermal event at *c.* 800 Ma which reset the Sm-Nd isotopic system in garnet-bearing assemblages in the Porthos Range of the nPCM. The significance of this poorly constrained age remains unclear, and it may yet prove to be a 'mixed' age between 1000 and 500 Ma. Whilst it is not inconceivable that part of the P–T history preserved in the Amery area is related an 800 Ma event, Hensen *et al.* (in press) suggest that evidence for this event is only recorded in the western half of the nPCM. In eastern Porthos Range, they obtained Sm-Nd ages of 630–500 Ma for garnet-bearing assemblages which they interpreted as reflecting Pan-African reworking. They concluded that the Pan-African overprint resulted in significant high grade metamorphism in the eastern nPCM, an interpretation which is consistent with the data from the Amery area and Fox Ridge.

Until detailed, structurally constrained geochronological work is done, the extent and nature of early Palaeozoic tectonism in the nPCM is difficult to gauge. In addition to the Sm-Nd chronological evidence for *c.* 500 Ma garnet corona development in the eastern Porthos Range (Hensen *et al.* in press), there is widespread resetting of Rb-Sr mineral systems throughout the nPCM (Arriens 1975, Tingey 1982). It seems

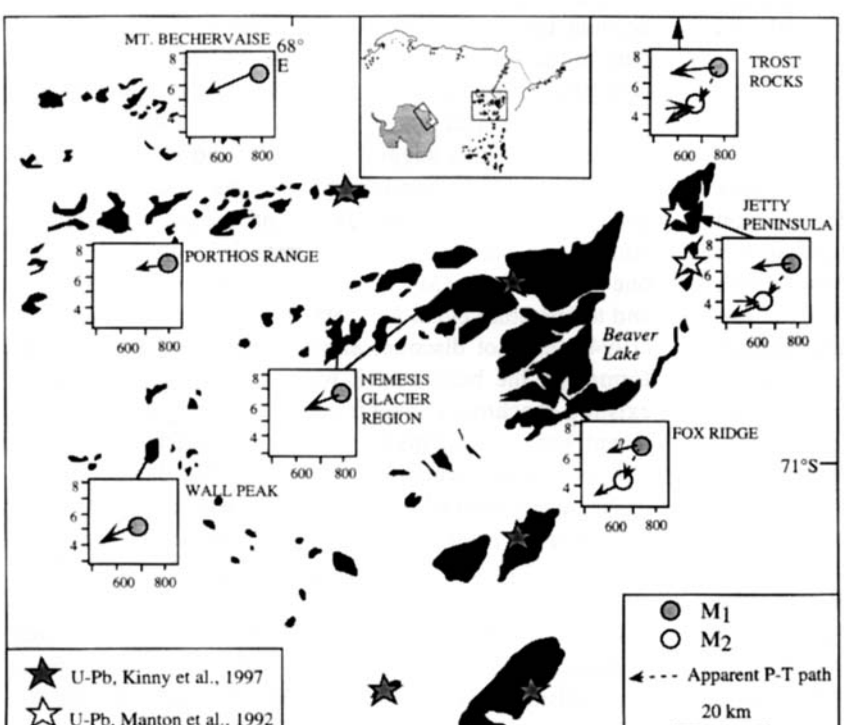

Fig. 8. Spatial distribution of PT paths in the nPCM and Amery area. The P–T trajectories from the nPCM are from Thost & Hensen 1992, Fitzsimons & Harley 1994a, 1994b, Nichols 1995, Hand 1996 unpub data). Also shown are the approximate locations of samples with undisturbed Proterozoic U-Pb systems (Kinny *et al.* 1997), and those with significant early Palaeozoic disturbance and new zircon and monazite growth (Manton *et al.* 1992). The inset shows the regional relationship between these areas and the early Palaeozoic granulite belt in Prydz Bay. The Proterozoic nPCM is dominated by near-isobaric cooling, whereas areas affected by renewed heating during the lower-P M_2 overprint are more closely linked with the region showing disturbed isotopic systems.

likely, however, that substantial exhumation of the nPCM occurred during the Early Palaeozoic, since M_2 pressures are *c.* 450 MPa and zircon fission track ages from the nPCM (Gleadow unpublished data, cited in Arne 1994) are also early Palaeozoic in age. The apparent absence of pervasive structural reworking in the nPCM during the early Palaeozoic suggests the region behaved as a relatively coherent block during exhumation. This is supported by peak *c.*1000 Ma pressures between 600–700 MPa across the entire nPCM (Fitzsimons & Thost 1992, Thost & Hensen 1992, Fitzsimons & Harley 1994a, 1994b, Hand unpublished data) suggesting partial reworking of the eastern margin of the terrain was not accompanied by significant differential exhumation. Although some deformation did accompany M_2 in the Amery and adjacent regions, early Palaeozoic reworking appears to have been a dominantly thermal process.

The interpretation that M_2 in the Amery area represents early Palaeozoic overprinting of a regional 1000 Ma terrain has significance for the wider class of questions regarding the interpretation of reaction textures in metamorphic rocks (e.g. Hand *et al.* 1992, Hensen *et al.* 1994, 1995, Vernon 1996). Since P–T paths only have relevance if they formed during a single event, the correct interpretation of the textural evolution of rocks is vital if they are to be used to infer processes relevant to orogenesis. In the Amery area, relatively anhydrous M_1 assemblages were overprinted by lower-T biotite-sillimanite-bearing assemblages which were subsequently destabilized to produce M_2 cordierite ± spinel assemblages. In rocks with a relatively anhydrous bulk composition, the M_1 assemblage was initially unreactive during M_2. However, close to peak M_2 conditions, re-equilibration of the M_1 assemblages proceeded along an apparent near-isothermal decompressional path (Fig. 6). The importance of recognizing the prograde nature of M_2 is that the decompressive P–T vector implied by the destabilization of M_1 assemblages in anhydrous rocks does not reflect the evolving metamorphic conditions, and is therefore misleading in its implications for the tectonic evolution of the region. While recognizing this aspect, the failure of Hand *et al.* (1994a) to appreciate the probable age difference between M_1 and M_2 (~ 450 Ma) lead to speculation that several shortlived granulite events where superimposed on a *c.* 1000 Ma exhumation path. While this may be true, the available evidence suggests otherwise.

Acknowledgements

We thank our fellow expeditioners on the 1989–90 and 1990–91 ANARE northern Prince Charles Mountains expeditions for their cooperation and assistance. Logistical support by the Australian Antarctic Division is gratefully acknowledged. This work was undertaken whilst I.S. was the recipient of an Australian Postgraduate Research Award. Mike Sandiford is thanked for his significant contributions during the course of this work and Chris Carson and Steve Boger are thanked for numerous fruitful conversations. We thank Ian Fitzsimons and Chris Carson for thorough and constructive reviews.

References

Andronikov, A.V. 1990. Spinel-garnet lherzolite nodules from alkaline ultrabasic rocks of Jetty Peninsula (East Antarctica). *Antarctic Science*, **2**, 321-330.

Aranovich, L.Ya. & Podlesskii, K.K. 1983. The cordierite-garnet-sillimanite-quartz equilibrium: experiments and applications. *In* Saxena, S.K., *ed. Kinetics and equilibrium in mineral reactions.* New York: Springer-Verlag, 173-198.

Arriens, P.A. 1975. Precambrian geochronology of Antarctica. *First Australian Geological Convention, Adelaide 1975, Abstracts*, 97-98. Geological Society of Australia.

Arne, A.C. 1994. Phanerozoic exhumation history of the northern Prince Charles Mountains (East Antarctica). *Antarctic Science*, **6**, 69-84.

Bhattacharya, A., Mazumdar, A.C. & Sen, S.K. 1988. Fe-Mg mixing in cordierite, constraints from natural data and implications for cordierite-garnet geothermometry in granulites. *American Mineralogist*, **73**, 338-344.

Bhattacharya, A., Krishnakumar, K.R., Raith, M. & Sen, S.K. 1991. An improved set of a-X parameters for Fe-Mg-Ca garnets and refinements of the orthopyroxene-garnet thermometer and the orthopyroxene-garnet-plagioclase-quartz barometer. *Journal of Petrology*, **32**, 629-656.

Bhattacharya, A., Mohanty, L., Maji, A., Sen, S.K. & Raith, M. 1992. Non-ideal mixing in the phlogopite-annite binary, constraints from experimental data on Mg-Fe partitioning and a reformulation of the biotite-garnet geothermometer. *Contributions to Mineralogy and Petrology*, **111**, 87-93.

Bohlen, S.R., Dollase, W.A. & Wall, V.J. 1986. Calibration and applications of spinel equilibria in the system $FeO-Al_2O_3-SiO_2$. *Journal of Petrology*, **27**, 1143-1156.

Bohlen, S.R., Wall, V.J., & Boettcher, A.L. 1983a. Geobarometry in granulites. *In* Saxena, S.K., *ed. Kinetics and equilibrium in mineral reactions.* New York: Springer-Verlag, 141-171.

Bohlen, S.R., Wall, V.J. & Boettcher, A.L. 1983b. Experimental investigations and application of garnet granulite equilibria. *Contributions to Mineralogy and Petrology*, **83**, 52-61.

Carson, C.J., Dirks, P.H.G.M., Hand, M., Sims, J.P. & Wilson, C.J.L. 1995. Compressional and extensional tectonics in low-medium pressure granulites from the Larsemann Hills, East Antarctica. *Geological Magazine*, **132**, 151-170.

Carson, C.J., Fanning, C.M. & Wilson, C.J.L. 1996. Timing of the Progress Granite, Larsemann Hills: evidence for Early Palaeozoic orogenesis within the east Antarctic Shield and implications for Gondwana assembly. *Australian Journal of Earth Sciences*, **43**, 539-553.

Clarke, G.L., Powell, R. & Guiraud, M. 1989. Low-pressure granulite facies metapelitic assemblages and corona textures from Mac. Robertson Land, East Antarctica: the importance of Fe_2O_3 and TiO_2 in accounting for spinel-bearing assemblages. *Journal of Metamorphic Geology*, **7**, 323-335.

Clemens, J.D. & Wall, V.J. 1981. Origin and crystallization of some peraluminous (S-type) granitic magmas. *The Canadian Mineralogist*, **19**, 111-131.

Dirks, P.H.G.M. & Hand, M. 1995. Clarifying P–T paths via structures in granulite from the Bolingen Islands, Antarctica. *Australian Journal of Earth Science*, **42**, 157-172.

Ellis, D.J., Sheraton, J.W., England, R.N. & Dallwitz, W.B. 1980. Osumilite-sapphirine-quartz granulites from Enderby Land, Antarctica; mineral assemblages and reactions. *Contributions to Mineralogy and Petrology*, **72**, 123-143.

ESSENE, E.J. 1989. The current status of thermobarometry in metamorphic rocks. *In* DALY, J.S., CLIFF, R.A. & YARDLEY, B.W.D., *eds. Evolution of metamorphic belts.* Geological Society of London Special Publication, No. 43, 1-44.

FITZSIMONS, I.C.W. 1996. Metapelitic migmatites from Brattsrand Bluffs, East Antarctica - metamorphism, melting and exhumation of the mid crust. *Journal of Petrology,* **37**, 395-414.

FITZSIMONS, I.C.W. & HARLEY, S.L. 1994a. Garnet coronas in scapolite-wollastonite calc-silicates from East Antarctica: the application and limitation of activity corrected grids. *Journal of Metamorphic Geology,* **12**, 761-777.

FITZSIMONS, I.C.W. & HARLEY, S.L. 1994b. The influence of retrograde cation exchange on granulite P–T estimates and a convergence technique for the recovery of peak metamorphic conditions. *Journal of Petrology,* **35**, 543-576.

FITZSIMONS, I.C.W., KINNY, P.D. & HARLEY, S.L. 1997. Two stages of zircon and monazite growth in anatectic leucogneiss: SHRIMP constraints on the duration and intensity of Pan-African metamorphism in Prydz Bay, East Antarctica. *Terra Nova,* **9**, 47-51.

FITZSIMONS, I.C.W. & THOST, D.E. 1992. Geological relationships in high-grade basement gneiss of the northern Prince Charles Mountains, East Antarctica. *Australian Journal of Earth Sciences,* **39**, 173-194.

GANGULY, J. & SAXENA, S.K. 1984. Mixing properties of aluminosilicate garnets: constraints from natural and experimental data and application to geothermo-baromentry. *American Mineralogist,* **69**, 88-97.

GRANT, J.A. 1985. Phase equilibria in partial melting of pelitic rocks. *In* ASHWORTH, J.R., *ed. Migmatites.* Glasgow: Blackie & Son, 86-144.

HAND, M., DIRKS, P.H.G.M., POWELL, R. & BUICK, I.S. 1992. How well established is isobaric cooling in Proterozoic orogenic belts? An example from the Arunta Inlier, central Australia. *Geology,* **20**, 649-652.

HAND M. & KINNY, P. 1996. SHRIMP constraints on Palaeozoic high-T exhumation in SW Prydz Bay, East Antarctica. *In Evolution of Metamorphic Belts.* Geological Society of Australia, Abstracts, No. 42, 61-62.

HAND, M., SCRIMGEOUR, I., POWELL, R., STÜWE, K. & WILSON, C.J.L. 1994a. Metapelitic granulites from Jetty Peninsula, East Antarctica: formation during a single event or polymetamorphism? *Journal of Metamorphic Geology,* **12**, 557-573.

HAND, M., SCRIMGEOUR, I., STÜWE, K., ARNE, D. & WILSON, C.J.L. 1994b Geological observations in high-grade mid-Proterozoic rocks from Else Platform, northern Prince Charles Mountains region, East Antarctica. *Australian Journal of Earth Sciences,* **41**, 311-329.

HARLEY, S.L. 1984. An experimental study of the partitioning of Fe and Mg between garnet and orthopyroxene. *Contributions to Mineralogy and Petrology,* **86**, 359-373.

HARLEY, S.L. & HENSEN, B.J. 1990. Archaean and Proterozoic high-grade terrains of East Antarctica (40-80°E): a case study of diversity in granulite facies metamorphism. *In* ASHWORTH, J.R. & BROWN, M., *eds. High-grade metamorphism and crustal anatexis.* London: Unwin Hyman, 320-370.

HARTE, B. & HUDSON, N.F.C. 1979. Pelite facies series and the temperatures and pressures of Dalradian metamorphism. *In* HARRIS, A.L., HOLLAND, C.H. & LEAKE, B.E., *eds. The Caledonides of the British Isles - reviewed.* Geological Society of London Special Publication, No. 8, 323-337.

HENSEN, B.J. 1971. Theoretical phase relations involving cordierite and garnet in the system MgO-FeO-Al_2O_3-SiO_2. *Contributions to Mineralogy and Petrology,* **33**, 191-214.

HENSEN, B.J. 1987. P–T grids for silica-undersaturated granulites in the system MAS (n+4) and FMAS (n+3): tools for the derivation of P–T paths of metamorphism. *Journal of Metamorphic Geology,* **5**, 255-271.

HENSEN, B.J. & GREEN, D.H. 1971. Experimental study of the stability of cordierite and garnet in pelitic compositions at high pressures and temperatures. I. Compositions with excess aluminosilicate. *Contributions to Mineralogy and Petrology,* **33**, 309-330.

HENSEN, B.J. & HARLEY, S.L. 1990. Graphical analysis of P–T-X relations in granulite facies metapelites. *In* ASHWORTH, J.R. & BROWN, M., *eds. High-grade metamorphism and crustal anatexis,* London: Unwin Hyman, 19-56.

HENSEN B.J. & ZHOU, B. 1995. A Pan-African granulite facies metamorphic episode in Prydz Bay, Antarctica: evidence from Sm-Nd garnet dating. *Australian Journal of Earth Sciences,* **42**, 249-258

HENSEN B.J., ZHOU, B. & THOST D. 1994. Two stage garnet breakdown in mafic gneisses from Antarctica: two granulite events confirmed by Sm-Nd dating (abstract). *In* BOYLE, A. & WHEELER, J., *eds. Controls of metamorphism.* Liverpool: University of Liverpool, 27.

HENSEN B.J., ZHOU, B. & THOST D. 1995. Are reaction textures reliable guides to metamorphic histories? Timing constraints from garnet Sm-Nd chronology for 'decompression' textures in granulites from Søstrene Island, Prydz Bay, Antarctica. *Geological Journal,* **30**, 261-271.

HENSEN B.J., ZHOU, B. & THOST D. in press. Recognition of multiple high-grade metamorphic events with garnet Sm-Nd chronology in the northern Prince Charles Mountains, Antarctica. *In* RICCI, C.A., *ed. The Antarctic region: geological evolution and processes.* Siena: Museo Nazionale dell'Antartide.

HODGES K.V. & CROWLEY, P.D. 1985. Error estimation and empirical geothermobarometry for pelitic systems. *American Mineralogist,* **70**, 702-709.

HODGES, K.V. & SPEAR, F.S. 1982. Geothermometry, geobarometry and the Al_2SiO_5 triple point at Mt. Moosilauke, New Hampshire. *American Mineralogist,* **67**, 1118-1134.

HOFMANN, J. 1991. Fault tectonics and megmatic ages in the Jetty Oasis area, Mac. Robertson Land: A contribution to the Lambert rift development. *In* THOMSON, M.R.A., CRAME, J.A. & THOMPSON, J.W., *eds. Geological evolution of Antarctica.* Cambridge: Cambridge University Press, 107-112.

HOLDAWAY, M.J. & LEE, S.M. 1977. Fe-Mg cordierite stability in high grade pelitic rocks based on experimental, theoretical and natural observations. *Contributions to Mineralogy and Petrology,* **63**, 175-198.

KAMENEV, E., ANDRONIKOV, A.V., MIKHALSKY, E.V., KRASNIKOV, N.N. & STÜWE, K. 1993. Soviet geological maps of the Prince Charles Mountains, East Antarctic Shield. *Australian Journal of Earth Sciences,* **40**, 501-517.

KINNY, P.D., BLACK, L.P. & SHERATON, J.W. 1993. Zircon ages and the distribution of Archaean and Proterozoic rocks in the Rauer Islands. *Antarctic Science,* **5**, 193-206.

KINNY, P.D., BLACK, L.P. & SHERATON, J.W. In press. Zircon U-Pb ages and geochemistry of igneous and metamorphic rocks from the northern Prince Charles Mountains, Antarctica. *Australian Journal of Earth Sciences.*

LAL, R.K. 1993. Internally consistent recalibrations of mineral equilibria for geothermobarometry involving garnet-orthopyroxene-plagioclase-quartz assemblages and their application to the South Indian granulites. *Journal of Metamorphic Geology,* **11**, 855-866.

LEE, H.Y. & GANGULY, J. 1988. Equilibrium compositions of coexisting garnet and orthopyroxene: experimental determinations in the system FeO-MgO-Al_2O_3-SiO_2 and applications. *Journal of Petrology,* **29**, 93-113.

MANTON W.I., GREW, E.S., HOFMANN, J. & SHERATON, J.W. 1992. Granitic rocks of the Jetty Peninsula, Amery Ice Shelf area, East Antarctica. *In* YOSHIDA, Y., KAMINUMA, K. & SHIRAISHI, K., *eds. Recent progress in Antarctic earth science.* Tokyo: Terra Scientific Publishing Company, 179-189.

MCKELVEY, B.C. & STEPHENSON, N.C.N. 1990. A geological reconnaissance of the Radok Lake area, Amery Oasis, Prince Charles Mountains. *Antarctic Science,* **2**, 53-66.

MIKHALSKY, E.V., ANDRONIKOV, A.V. & BELIATSKY, B.V. 1992. Mafic igneous suites in the Lambert rift zone. *In* YOSHIDA, Y., KAMINUMA, K. & SHIRAISHI, K., *eds. Recent progress in Antarctic earth science.*

Tokyo: Terra Scientific Publishing Company, 173-178.

NEWTON, R.C. & HASSELTON, H.T. 1981. Thermodynamics of the garnet-plagioclase-Al2SiO5-quartz geobarometer. *In* NEWTON, R.C., NAVROTSKY, A. & WOOD, B.J., *eds. Thermodynamics of minerals and melts.* New York: Springer Verlag, 131-147.

NEWTON, R.C. & PERKINS III, D. 1982. Thermodynamic calibration of geobarometers based on the assemblages garnet-plagioclase-orthopyroxene (clinopyroxene)-quartz. *American Mineralogist,* **67,** 203-222.

NICHOLS, G.T. 1995. The role of mylonites in the uplift of an oblique lower crustal section, East Anarctica. *Journal of Metamorphic Geology,* **13,** 223-228.

NICHOLS, G.T, BERRY, R.F. & GREEN, D.H. 1992. Internally consistent gahnitic spinel-cordierite garnet equilibria in the FMASHZn system: geothermobarometry and applications. *Contributions to Mineralogy and Petrology,* **111,** 362-377.

PATTISON, D. & HARTE, B. 1985. A petrogenetic grid for pelites in the Ballachulish and other Scottish thermal aureoles. *Journal of the Geological Society of London,* **142,** 7-28.

PERCHUK, L.L. & LAVRET'EVA, I.V. 1983. Experimental investigation of exchange equilibria in the system cordierite-garnet-biotite. *In* SAXENA, S.K., *ed. Kinetics and equilibrium in mineral reactions.* New York: Springer-Verlag, 199-239.

PERKINS, D. & CHIPERA, S.J. 1985. Garnet-orthopyroxene-plagioclase-quartz barometry: refinement and application to the English River subprovince and the Minnesota River valley. *Contributions to Mineralogy and Petrology,* **89,** 69-80.

POWELL, R. & HOLLAND, T.J.B. 1988. An internally consistent dataset with uncertainties and correlations: 3. Applications to geobarometry, worked examples and a computer program. *Journal of Metamorphic Geology,* **6,** 173-204.

POWELL, R. & HOLLAND, T.J.B. 1994. Optimal geothermometry and geobarometry. *American Mineralogist,* **79,** 120-133.

SCRIMGEOUR, I. 1994. *Evolution of granulites from Mac. Robertson Land, East Antarctica.* PhD. thesis, University of Adelaide, 196 pp. [Unpublished.]

SENGUPTA, P., DASGUPTA, S., BHATTACHARYA, P.K. & MUKHERJEE, M. 1990. An orthopyroxene-biotite geothermometer and its application in crustal granulites and mantle derived rocks. *Journal of Metamorphic Geology,* **8,** 191-197.

SENGUPTA, P., KARMAKAR, S., DASGUPTA, S. & FUKUOKA, M. 1991. Petrology of spinel granulites from Araku, Eastern Ghats, India, and a petrogenetic grid for sapphirine-free rocks in the system FMAS. *Journal of Metamorphic Geology,* **9,** 451-459.

SHERATON, J.W., TINDLE, A.G. & TINGEY, R.J. 1996. Geochemistry, origin and tectonic setting of granitic rocks of the Prince Charles Mountains, Antarctica. *AGSO Journal of Australian Geology and Geophysics,* **16,** 345-370.

SHIRAISHI, K., ELLIS, D.J., HIROI, Y., FANNING, C.M., MOTOYOSHI, Y. & NAKAI, Y. 1994. Cambrian orogenic belt in East Antarctica and Sri Lanka: Implication for Gondwana assembly. *Journal of Geology,* **102,** 47-65.

THOMPSON, A.B. 1976. Mineral reactions in pelitic rocks: I. Prediction of P-T-X (Fe-Mg) phase relations. II. Calculation of some P-T-X (Fe-Mg) phase relations. *American Journal of Science,* **276,** 401-454.

THOST, D.E. & HENSEN, B.J. 1992. Gneisses of the Porthos and Athos Ranges, northern Prince Charles Mountains, East Antarctica: constraints on the prograde and retrograde P-T path. *In* YOSHIDA, Y., KAMINUMA, K. & SHIRAISHI, K., *eds. Recent progress in Antarctic earth science.* Tokyo: Terra Scientific Publishing Company, 93-102.

TINGEY, R.J. 1982. The geologic evolution of the Prince Charles Mountains-an Antarctic Archaean cratonic block. *In* CRADDOCK, C., *ed. Antarctic geoscience.* Madison: University of Wisconsin Press, 455-464.

VERNON, R.H. 1996. Problems with inferring P-T-t paths in low-P granulite facies rocks. *Journal of Metamorphic Geology,* **14,** 143-153.

WATERS, D.J. 1991. pHercynite-quartz granulites, phase relations, and implications for crustal processes. *European Journal of Mineralogy,* **3,** 367-386.

XU, GUOWEI, WILL, T.M. & POWELL, R. 1994. A calculated petrogenetic grid for the system K_2O-FeO-MgO-Al_2O_3-SiO_2-H_2O, with particular reference to contact-metamorphosed pelites. *Journal of Metamorphic Geology,* **12,** 99-119.

YOUNG, D.N. & BLACK, L.P. 1991. U-Pb zircon dating of Proterozoic igneous charnockites from the Mawson Coast, East Antarctica. *Antarctic Science,* **3,** 205-216.

ZHAO, Y., SONG, B., WANG, Y., REN, L., LI, J. & CHEN, T. 1992. Geochronology of the late granite in the Larsemann Hills, East Antarctica. *In* YOSHIDA, Y., KAMINUMA, K. & SHIRAISHI, K., *eds. Recent progress in Antarctic earth science.* Tokyo: Terra Scientific Publishing Company, 155-161.

ZHAO, Y., SONG, B., WANG, Y., REN, L., LI, J. & CHEN, T. 1995. Constraints on the stratigraphic age of metasedimentary rocks of the Larsemann Hills, East Antarctica, possible implications for Neo-Proterozoic tectonics. *Precambrian Research,* **75,** 175-188.